THESIS FOR THE DEGREE OF LICENTIATE OF ENGINEERING

Investigation of La promoted Pd/BEA Performance for Passive NO_x adsorption processes

Rojin Feizie Ilmasani

Chemical Engineering Division
Department of Chemistry and Chemical Engineering

CHALMERS UNIVERSITY OF TECHNOLOGY

Gothenburg, Sweden 2020

Investigation of La promoted Pd/BEA performance for Passive NO_x adsorption processes

Rojin Feizie Ilmasani

Licentiatuppsatser vid Institutionen för kemi och kemiteknik
Chalmers tekniska högskola.
Nr 2020:05.

Department of Chemistry and Chemical Engineering
Chalmers University of Technology
SE-412 96 Gothenburg
Sweden
Telephone + 46 (0)31-772 1000

Printed by Chalmers Reproservice
Gothenburg, Sweden 2020

Investigation of La promoted Pd/BEA performance for Passive NO_x adsorption processes

Rojin Feizie Ilmasani

Department of Chemistry and Chemical Engineering
Chalmers University of Technology, Gothenburg 2020

Abstract

Lean-burn combustion engines have been used to improve fuel efficiency by reducing fuel consumption. However, these engines face challenges in lean reduction of NO_x for exhaust after-treatment systems. Therefore, two common techniques are applied for lean-burn gasoline engines and diesel engines to reduce emitted NO_x, which includes selective catalytic reduction (SCR) and lean NO_x traps (LNT). However, both techniques have limitations at exhaust temperatures below 200°C which can be problematic for them to achieve ultra-low NO_x emissions. Thus, Passive NO_x adsorber (PNA) have been suggested for preventing cold-start NO_x emissions. In this method, NO_x is trapped at low temperatures onto the adsorbent and is later released at exhaust temperatures higher than 200°C. The released NO_x can be reduced by the following SCR or LNT unit at higher temperatures. One of the well-known adsorbents in PNA, has been Pd on zeolites due to its high NO_x storage capacity. One important aspect is that the NOx desorption should not occur before the light-off temperature has been reched in the SCR or LNT. In this work, Ce, Zr and La have been used as promoters for Pd/BEA. Among these materials, La promotion was shown to efficiently increase the NO_x desorption temperature above 200°C compared with the reference material. Furthermore, the effect of water and hydrogen pretreatment was studied for La-Pd/BEA and the reference material Pd/BEA. The results indicated that, the presence of water blocked the adsorption of weakly adsorbed NO on the samples which shifted the desorption temperatures to higher values (>200°C). On the other hand, hydrogen pre-treatment had a negative effect on NO_x trap capacity and desorption temperature. Interestingly, the La promoted sample was less sensitive to H_2 pre-treatment. Characterization methods such as TPO and XPS, indicated that the La promoted sample consisted of more stable Pd oxides which needed higher temperatures to desorb O_2. DRIFTS analysis showed that NO was adsorbed in the form of more strongly bound species (nitrates) in greater quantities with La promotion compared with the reference sample. In addition, the effect of multiple cycles of NO TPD experiments were studied with elevated levels of CO in the inlet gas, to compare the performance and stability of the La promoted and reference materials. The La promoted adsorbent showed stable behavior in NO_x desorption beyond a 5^{th} cycle while the NO_x storage increased at around 160°C with each cycle. Whereas, a stronger degrading behavior was observed for the Pd/BEA sample where NO_x storage and desorption decreased with each TPD cycle. The same pattern was observed in DRIFTS analysis with the types and relative quantities of NO_x adsorbed species for each material. O_2-TPD analysis indicated more Pd clusters formed on the unpromoted material compared with the promoted one with the presence of CO during multiple NO TPD experiments. This caused a degradation in NO_x release from the unpromoted material due to its decreasing content of ion-exchange Pd which is considered the main NO_x adsorption site at low temperatures.

Keywords: *PNA, Pd/BEA, Lanthanum, Ceria, Zirconium, CO effect, NO TPD.*

Acknowledgements

This work is performed at Chemical Engineering and Competence Centre for Catalysis. The Swedish Research Council is gratefully acknowledged for the financial support.

I would also like to thank:

- My main supervisor Professor Louise Olsson for all your support, ideas and encouragement. I am very lucky to have the chance of being your student and be a part of your research group.
- My co-supervisor and examiner Derek Creaser for all your valuable help, valuable discussions and inputs. It has been such a pleaser to have you in my research.
- Jungwon Woo and Aiyong Wang for all the support and valuable discussions.
- My office mates, Jesus and Ida for amazing discussions and wonderful moments that we shared every day.
- Stefan Gustafsson and Eric Tam for your help with TEM and XPS measurements.
- Malin Larsson and Anna Oskarsson for providing administrative support.
- Lasse Urholm and Lennart Norberg for all the help in the reactor lab.
- All my current and former co-workers at KCK for all the fun, discussions and wonderful moments.
- My lovely family for all their never-ending support and love that they give me every moment of my life. Love you all so much.
- And finally, to all the doctors and nurses who are sacrificing their lives and families to give us a safer world to breath in. Humanity will never forget their brave souls for fighting COVID-19.

List of publications

I. Influencing the NO_x stability by metal oxide addition to Pd/BEA for passive NO_x adsorbers

Rojin Feizie Ilmasani, Jungwon Woo, Derek Creaser, Louise Olsson
Submitted.

II. Investigation of CO deactivation of passive NO_x adsorption on La promoted Pd/BEA

Rojin Feizie Ilmasani, Aiyong Wang, Derek Creaser, Louise Olsson
Manuscript

Contribution report

Paper I

I synthesized the catalyst samples, performed the catalyst characterizations (except STEM and EDX, and ICP-SEMS), conducted the flow reactor experiments, interpreted the results together with my co-authors and was responsible for writing the manuscript.

Paper II

I synthesized the catalyst samples, performed the catalyst characterizations (except STEM and EDX, XPS and ICP-SEMS), conducted the flow reactor experiments, interpreted the results together with my co-authors and was responsible for writing the manuscript.

List of abbreviations

BET	Brunauer Emmat Teller
CEM	Controller Evaporator and Mixer
DRIFTS	Diffuse Reflectance Infrared Fourier Transform Spectroscopy
FTIR	Fourier Transform Infrared Spectroscopy
MS	Mass Spectrometer
MFC	Mass Flow Controller
PNA	Passive NOx adsorbents
SAR	Silica to Alumina Ratio (molar ratio SiO_2/Al_2O_3)
TEM	Transmission Electron Microscopy
TPD	Temperature Programmed Desorption
TPO	Temperature Programmed Oxidation
XPS	X-ray Photoelectron Spectroscopy

Contents

1 Introduction 1
1.1 Background 1
1.2 Objectives 3
2 Passive NO_x adsorbents 5
2.1 Key factors in PNAs 5
2.2 NO adsorption and desorption 6
2.2.1 Exhaust species 8
2.2.2 Promoters 9
2.2.3 Hydrothermal aging and pretreatment 9
3 Experiments and equipment 11
3.1 Sample synthesis 11
3.1.1 Pd/BEA as a reference sample 11
3.1.2 Promoted 1%Pd/BEA 12
3.1.3 Monolith preparation 13
3.2 Flow reactor and NO adsorption/desorption activity 14
3.3 Characterization techniques 15
3.3.1 Inductively coupled plasma sector field mass spectrometry (ICP-SFMS) 15
3.3.2 Specific surface area analysis (BET) 15
3.3.3 Transmission electron microscopy (TEM) 16
3.3.4 X-ray photoelectron spectroscopy (XPS) 17
3.3.5 Temperature programmed experiments 17
3.3.6 In-situ DRIFT Spectroscopy 18
4. Results and discussion 21
4.1 Flow reactor results 21
4.1.1 Study of different promoters on Pd/BEA and hydrogen pre-treatment effect 21
4.1.2 Varying La loading and H_2O effect 23
4.1.3 CO effect on sequential passive NO_x adsorption 24
4.2 Physicochemical characterization 26
4.3 DRIFT spectroscopy 32
5. Conclusions and outlook 35
6. References 37

1 Introduction

1.1 Background

Fulfilment of the needs in today's modern society, needs conversion of sufficient amounts of energy for transportation, heating and industry activities. This energy is partly generated by combustion of various fuels which leads to release of exhaust gases, causing air pollution effects. Green-house gas emissions i.e. carbon dioxide, is one of the main emissions from combustion of non-renewable fuel[1-2]. In 2015, the transportation sector, which has been growing rapidly since the 1970s, was the second largest contributor after power generation sector for greenhouse gas emissions due to CO_2 [2-5]. Consequently, for higher fuel efficiency and lower CO_2 emissions, lean-burn gasoline and diesel engines have been introduced[6]. These engines use higher air-to-fuel ratio (AFR) compared with regular engines, which results in more efficient combustion by utilization of the fuel to a higher extend [7]. Although the lean-burn combustion concept is beneficial for improvement of fuel economy, however, NO_x reduction over a three-way (TWC) catalyst to N_2, in an oxygen-rich environment is not possible[8-9]. NO_x emissions are harmful and toxic, and they can cause environmental, ecological and health threats[10-11]. Therefore, strict regulations are placed on emissions of nitrogen oxides (NO_x)[12]. Hence, the development of an effective and economical catalyst system which can control NO_x emissions in lean exhaust steam is required.

Nitrogen oxides (NO_x) is a general term for NO and NO_2 which are highly reactive and poisonous gases. NO_x emissions can react in the atmosphere to form ozone (O_3), acidic rain and smog[10, 13]. NO_x formation in diesel engines, can occur when the temperature of combustion chamber exceeds 2000 K (denoted as thermal NO_x), or NO_x can form by oxidation of already-ionized nitrogen compounds in the fuel (fuel NO_x) or from combination of nitrogen molecules in the air with fuel (prompt NO_x)[14]. NO_x emissions can cause biological problems for human beings including respiratory diseases such as asthma, pneumonia and bronchitis[11].

Therefore, it is important to develop different techniques for controlling NO_x emissions according to the worldwide regulations to preserve public health and welfare.

To achieve high NO_x reduction efficiency, selective catalyst reduction (SCR) and Lean NO_x trap (LNT) are commonly applicable techniques in lean-burn engines[15-16]. However, both methods have their own limitations at cold-start conditions. With SCR systems, a continuous selective catalytic reduction of NO_x to N_2 and H_2O occurs through reaction with NH_3. However, due to that urea is a liquid it is preferred to use, where the urea is decomposed at high temperature (>200℃) and hydrolysis to form NH_3. The present limitation with SCR method is at low engine operating temperatures (<200℃), where the urea decomposition has very low rate [17-18], which results in that urea injection is not possible. On the one hand, LNT has been introduced using lean/rich cycles (oxygen excess/fuel excess), in which NO_x is trapped under lean condition in the forms of nitrates and nitrites on a storage compound. After saturation of storage compound (under rich condition), the catalyst will be regenerated [19-20]. However, in this method, low temperature operating conditions cause lower efficiency in oxidizing NO to NO_2[21-22], which thereby reducing the NO_x trapping efficiency. Also, the regeneration of the stored NO_x is limited at low temperature.

To control emitted NO_x in the cold-start, multiple adsorbents were examined with the ability of temporarily storing NO_x at low temperature and then releasing NO_x by increasing the temperature. This method has been called as passive NO_x adsorbers (PNA), which is intended to be located upstream of the SCR catalyst. In this method, NO_x should be adsorbed at low temperatures and while ramping up to higher engine temperatures NO_x will be desorbed. The goal is that the NO_x release should be above 200℃ (urea dosing temperature), in order to facilitate the removal of NO_x in the SCR system. Many studies have confirmed that supported noble metals (Pd, Pt and Ag) supported on alumina/ceria are promising adsorbents[17, 23-24]. However, the high large sulfur poisoning of these adsorbents resulted in a great interest on materials with zeolite supports mostly with Pd as noble metal[22, 25]. However, to our knowledge there are no published studies in the literature which focus on the effect of promoters' on Pd/zeolite materials. Concerning studies for PNA applications, the effect of CO on the activity of the adsorbent has been shown to be beneficial for the NO_x storage amount and the NO_x release temperature[26]. However, recent studies have shown that the presence of CO during long-term sequential NO_x adsorption and desorption is severely deactivating the Pd/zeolite material[27-28].

1.2 Objectives

The objective of this thesis is to fundamentally investigate the performance of Pd/Zeolite-base adsorbents with various promoters, regarding the desorption temperature range and stability during sequential NO TPD. More specifically, in the first part of the study, Ce, Zr and La were studied as promotes on 1%Pd/BEA zeolite (SAR of 38). Thereafter, the behavior of the La promoted sample directed us to further study varying concentrations of lanthanum on the PNA process. Knowing the storage degrading behavior of Pd/BEA after multiple NO_x adsorption/desorption cycles in the presence of CO, led us to investigate the performance of a La promoted Pd/BEA sample in the same condition. In both studies, Pd/BEA was used as a reference sample. Various characterization techniques were used combined with a flow reactor set up in order to fundamentally understand the effect of La as a promoter in PNA processes.

2 Passive NO_x adsorbents

In diesel engines, the passive NO_x adsorbents are intended to adsorb NO_x emissions during cold-start periods in the existing after-treatment systems. The cold-start period can be generally referred to as the very first few minutes when the engine starts operating after a long continuous shut-down, until the catalyst has reached its operating temperature. Thus, PNA is an interesting technique, since it can store the NO_x at low temperature during cold-start[29]. The engine temperature eventually exceeds 180-200°C (the minimum urea dosing temperature) and at this temperature NO_x reduction catalysts can begin to operate efficiently. Therefore, the adsorber should ideally begin to release NO_x after 200°C.

2.1 Key factors in PNAs

The adsorbers in the PNA processes are evaluated based on different factors. Some of these factors include:

- NO_x storage capacity at low temperatures
- Desorption temperature
- Degradation resistance

Generally the adsorbent storage at a certain temperature is calculated by considering the amount of adsorbed NO_x molecules per unit mass of the adsorbent[30]. Basically, greater NO_x adsorption at low temperatures is more desirable in order to have efficient performance and minimize the amount of adsorbent required for trapping the cold-start NO_x. The desorption temperature is referred to the gas temperature where the adsorbed NO_x begins to be released during heating of the catalyst. The desorption temperature range can vary for different materials, but it is most preferable if the desorption starts not lower than 200°C and is completed not higher than 400°C[25, 29, 31-34]. Degradation occurs for PNAs due to several thermal

aging and poisoning conditions. This degradation can appear either as alower NO_x storage capacity and correspondingly desorption quantity or it could result in a shift of the adsorption/desorption temperature to non-optimal ranges. Degradation can be a crucial factor affecting the lifetime of the PNA. Thus, it is important to monitor these deviations that can occur during PNA experiments.

2.2 NO adsorption and desorption

Produced NO_x at low temperature is generally in the form of NO in the exhaust gases, thus the NO adsorption is in focus for PNAs. Supported precious materials such as Pt, Pd and Ag are the most studied materials as adsorbents for PNA processes[17, 22-23, 25, 30, 35]. Crocker et al. studied alumina and ceria base materials with Pt and Pd, and they found a superior NO_x adsorption performance in the presence of Pt and Pd in the adsorbents[17, 24, 36]. In another study, Chen et al. showed a significant low temperature NO_x storage capacity for $Pt/Pd/CeO_2$ with various loadings of Pt and Pd[30]. According to a study by Ryou et al., the performance of Pd/CeO_2 was better than Pt/CeO_2 and $Pt/Pd/CeO_2$ based PNAs[34]. However, later reports in the literature, showed that these materials can undergo a severe degradation in NO_x storage capacity due to sulfur poisoning[22-23, 37].

Subsequently, new attempts shifted to zeolite base materials. Chang et al. assessed the performance of Ca-beta zeolites and showed an increase in NO_x trapping with this material. They also reported that when increasing the amount of loading of CaO from 5 to 10 wt.%, the penetration time (required time for NO to be detected in reactor outlet during adsorption) increased from 38 to 51 min[38]. Chen et al. studied Pd-SSZ-13 and Pd/BEA with more practical exhaust conditions where CO, water and $nC_{10}H_{22}$ were present. They also studied the sulfated materials in the same condition and it was reported that the ability of NO_x uptake for all the samples was almost the same, even after the poisoning[22]. Many other studies have been done in more detail regarding Pd based zeolites and more specifically Pd/BEA and all showed a significant storage capacity in PNA experiments [25-26, 39]. Therefore, it appears that Pd has become the first choice of precious metals for PNAs and highest NO_x storage was achieved for loadings of ~1 wt.% Pd [22, 26]. Concentrations higher than 1 wt.% for Pd limits the dispersion of Pd cations, thus it is critical to achieve high ion-exchange levels.

Generally, Pd particles on zeolite supports for PNA processes can be in three forms including clusters, nanoparticles and ion-exchanged metal sites[25, 40-42]. Pd clusters have larger particle sizes compared with pore size of the support, therefore these are easily detected

on the surface of the support[25]. Pd nanoparticles can be smaller than the support's pore size, hence they can be located both inside and outside the pores of the support[42]. These nanoparticles can range between 2-5 nm in size[21]. Ion-exchange Pd sites can form due to an interaction of Pd atoms and Brønsted acid sites, which can form between a proton in acid sites and a metal cation[43]. For adsorption of NO_x both ionic Pd and PdO_x can be efficient under dry condition. According to Zheng et al. NO_x trapping and release are complex chemisorption and desorption events, involving complicated chemical reactions. The below equations are simplified suggested reactions for NO trapping under dry conditions (Z^- represents a cationic exchange site) [25]:

$$Z^-Pd^{2+}Z^- + NO \rightarrow Z^-Pd^{2+}(NO)Z^- \quad (1)$$

$$3NO + 2Z^-[Pd(II)OH)]^+ \rightarrow 2Z - Pd^+(NO) + NO_2 \quad (2)$$

$$Pd(IV)O_2 + 2NO \rightarrow (NO)Pd(II)O + NO_2 \quad (3)$$

In this case Pd(IV) can reduce to Pd(II) during NO adsorption and then later the formed Pd(II) can become another adsorption site. However, Zheng et al. also reported that the ability of NO_x adsorption with Pd(IV), will be reduced in the presence of water[25].

Moreover, results by Chen et al. showed that hydrothermal aging caused the PdO particles to transform to ionic Pd which increased the NO_x storage capacity for Pd/zeolite base materials[31]. Therefore, it has been found that ionic Pd^{2+} particles are the main NO_x adsorption sites at low temperatures in the presence of water [22].

After isothermal NO_x storage, a temperature programmed desorption is applied to investigate the desorption properties of the adsorbent. The desorption temperature window should start at a specific temperature in which the downstream NO_x reduction catalyst can begin to be active. In the case of NH_3-SCR systems, the required minimum desorption temperature is 200°C[16, 44]. Desorption at too low temperatures causes ineffective NO_x reduction and on the other hand, too high temperature release can inhibit regeneration or removal of NO_x in the further cycles[26, 45]. Many important factors can affect the adsorption and desorption properties in PNA processes which are listed as follow.

2.2.1 Exhaust species

Exhaust from lean-burn engines generally contains many species aside from NO_x. These additional species include O_2, N_2, CO, H_2O, hydrocarbons and CO_2. N_2 has no effect on the adsorption and desorption of NO_x due to its inert properties. It has been reported by Khivantsev that oxygen can have an effect on PNA specially in Pd-zeolite adsorbents by activating an extra NO adsorption bond due to formation of nitrates[42]. The presence of CO_2 has been shown to have a negative impact on NO_x adsorption for non-zeolite based adsorbents which can be due to formation of carbonates and their competition with NO_x for adsorption sites[24]. However, according to Vu et al. CO_2 has no effect on NO_x adsorption with Pt/Pd zeolite supports[26].

The effect of H_2O has been studied in many papers, and all results show that water severely reduces NO_x storage at low temperatures and this is due to blockage of Brønsted acid sites by H_2O molecules[21, 25, 46-47] and also due to blockage of the Lewis acid sites such as Pd. Correspondingly, lower NO_x adsorption in the presence of water leads to lower desorption as well. Theis et al. showed that the presence of water suppressed the NO_x trapping capacity at low temperatures (<100°C) for both Pd and Pt on Al_2O_3 or CZO (ceria zirconia mixed oxide). This was due to the condensation of water on the storage sites[48].

Various studies indicated that CO can improve the NO_x storage capacity and reduce the negative effects of H_2O either by Pd reduction or by formation of nitrogen-carbon-oxygen species[25, 47-48]. Vu et al. examined the effect of different concentrations of CO (from 0-225 ppm) and it was observed that by increasing the quantity of CO larger NO_x desorption could be achieved for Pd/BEA[26]. Also it was observed that the desorption peaks at low temperatures (<200°C) for Pd/BEA was shifted to higher temperature values with CO due to more stable Pd oxidation states[26]. This is a beneficial effect for PNA processes for the cases where the desorption was at temperatures below urea dosing. In addition, it was also reported that at higher temperatures (>200°C) the release peak had shifted to lower values (still higher than 200°C) [47].

It is important to mention that for vehicle engines, there can be multiple cold-start steps, thus it is important to know how the PNAs behavior will be after several NO_x adsorption/desorption cycles. Correspondingly, very recent studies by Yuntao and Thesis et al. indicated that repeated NO_x storage and release cycles with CO, can cause a gradual degradation for NO_x adsorption and desorption with Pd/Zeolite materials [27-28].

2.2.2 Promoters

It has been a few studies on the addition of promoters to PNA systems. Ji et al. studied La promoted Pt/Al_2O_3 performance for PNA processes while they investigated different concentrations of La for the adsorbent. They reported that the presence of La enhanced the formation of nitrate bonds[24]. In another study, Crocket et al. studied different promoters for Pt/Pd/metal oxide in which it was mentioned that the lanthanum group metals showed a beneficial behavior for Pt/Pd/metal oxide materials for PNA processes[36]. Jones et al. also studied the effect of various promoters including La group metals on Pt/CeO_2 and Pd/CeO_2 and they reported a positive effect of Pr as a promoter in adsorption and desorption of NO_x[17]. However, to our knowledge there are no published studies available that examine the effects od promoters to Pd/zeolites.

2.2.3 Hydrothermal aging and pretreatment

Ryou et al. showed that the hydrothermal aging (HTA) of Pd/SSZ-13, enhanced the NO storage performance at low temperatures. They found that HTA can be helpful in the temperature range of 700-750°C, however going to temperatures higher than 850°C, causes agglomeration of Pd particles that reduces the storage capacity. According to H_2-TPR they claimed that this enhancement by HTA is due to an increased distribution of PdO into highly dispersed Pd^{2+} species within the zeolite structure[31-32]. This was also reported by Okumura et al. for Pd supported on ZSM-5[49].

In many studies prior to the NO_x storage and release step, a pre-treatment step takes place in order to ensure complete removal of all NO_x residuals from the adsorbent. The pre-treatment step consists of a reducing agent such as H_2 along with O_2 and H_2O at high temperature. The pre-treatment step with hydrogen can have an important effect on the nature of the Pd oxidation state[40]. At sub-ambient temperatures, hydrogen can reduce PdO_x particles and also form PdH, and at higher temperatures, Pd ionic species can become reduced to lower oxidation states[50]. In another study, a higher mobility of reduced Pd species was observed which can lead to Pd agglomeration on the surface[43]. Therefore, H_2 pre-treatment can have undesirable effects on Pd containing PNAs.

3 Experiments and equipment

The performance and stability of the PNA adsorbents were investigated in this study. Initially the adsorbent performance was studied in flow reactor experiments followed by detailed characterizations for better understanding of the reactor results. These characterizations methods included, BET, STEM, XPS, TPO, O_2-TPD and in-situ DRIFTS analysis. The synthesis of the samples and the characterization methods will be described in the following sections.

3.1 Sample synthesis

3.1.1 Pd/BEA as a reference sample

In all samples, Pd has been used with Beta zeolite support and Pd has been deposited by an "incipient wetness impregnation method" on the support material (in both **Paper I** and **Paper II**). All the results were compared with a prepared reference sample consisting of 1 wt.% Pd loaded on Beta zeolite support. For preparation of samples, a diluted Pd precursor solution of palladium (II) nitrate (Sigma-Aldrich, 4-5 wt.% Pd) and commercial Beta Zeolite (CP814C, SAR (SiO_2-to-Al_2O_3 molar ratio) 38, form Zeolyst International) were used. However, in **Paper I** the material loading was started with promoters (Section 3.1.2) followed by impregnation of Pd on promoted Beta support. Thereafter, in **Paper II** the promoted sample was prepared with a reverse sequence.

Incipient impregnation method

For preparation of the samples with this method, a corresponding amount of $Pd(NO_3)_2$ solution (for 1 wt.% loading) was diluted in a specific amount of MilliQ water (Millipore). The amount of water is related to the total pore volume of the support material. The solution was added dropwise to the support material (Beta zeolite SAR 38) and was fully mixed

with a spatula. Afterwards, the powder was dried at 100℃ overnight, followed by calcination at 500℃ for 5 h reached with the use of a temperature ramping rate of 2℃/min.

3.1.2 Promoted 1%Pd/BEA

The studied promoters in **Paper I** consisted of ceria (Ce), zirconium (Zr) and lanthanum (La) with loadings of 10 wt.%. The commercial precursors were, cerium (III) nitrate hexahydrate (Sigma-Aldrich), zirconium (IV) oxynitrate hydrate (Sigma-Aldrich) and lanthanum (III) nitrate hydrate (Sigma-Aldrich) respectively. For preparation of these three samples, first the promoters were impregnated on the Beta zeolite and then Pd was loaded on the next step on the promoted support. The target concentration loading for promoters (10 wt.%) was achieved in two steps of 5 wt.% deposition by an incipient wetness impregnation method. After each loading step the powder was dried at 100℃ overnight and then finally after reaching 10 wt.% loading of the promoter the calcination at 500℃ for 5 h followed the drying step. Thereafter, the promoted zeolite was impregnated with Pd solution to reach 1 wt.% loading and further dried and calcined in the same manner. Furthermore, in **Paper I**, different concentrations of La ranging from 2.7-10 wt.% was studied. The synthesis of these samples started with a large batch of 2.7 wt.% La loaded on the zeolite support. After drying overnight, higher concentrations of La were gradually loaded in further steps and in each step the sample was dryed at 100℃ overnight. Samples with 2.7, 3.5, 5.4, 7.0 and 10.0 wt.% La were calcined at 500℃ for 5 h following a temperature ramping at 2℃/min. Eventually, 1 wt.% Pd was deposited on the promoted zeolite samples.

In **Paper II** three different samples were studied, including 1 wt.%Pd/BEA as a reference sample and two La promoted samples (2.7wt.% La) with opposite La loading sequences. These samples were prepared with the same incipient wetness method as before. All prepared samples are listed in Table 1 and 2 and they are named respective to the loading sequence of metals on BEA zeolite. For example, in 2.7%La-Pd/BEA, La was loaded first on the support before Pd.

Table 1. List of prepared samples in **Paper I**.

Adsorbent Material	Metal Loading (wt.%)[1]			
	Pd	**Ce**	**Zr**	**La**
Pd/10%Ce/BEA	0.9	10.0	-	-
Pd/10%Zr/BEA	0.9	-	10.0	-
Pd/10%La/BEA	1.0	-	-	10.0
Pd/7%La/BEA	0.9	-	-	7.0
Pd/5.4%La/BEA	0.9	-	-	5.4
Pd/3.5%La/BEA	1.0	-	-	3.5
Pd/2.7%La/BEA	0.9	-	-	2.7
Pd/BEA	0.9	-	-	-

[1] Specified loadings are based on ICP-SFMS analysis of the prepared adsorbent materials.

Table 2. List of prepared samples in Paper II.

Adsorbent Material	Metal Loading (wt.%)	
	Pd	**La**
2.7%La-Pd/BEA	0.9	2.7
Pd-2.7%La/BEA	1.1	2.7
Pd/BEA	1.1	-

3.1.3 Monolith preparation

The samples were washcoated on honeycomb structured cordierite monoliths (cpsi of 400) for flow reactor measurements. All the monoliths were cut to a length of 2 cm and diameter of 2.1 cm and to remove contaminants, they were heated at 550℃ for 2 h in air. The prepared slurry for coating contained a 90:10 mass ratio of the liquid to solid phase. The solid phase contained the sample powder and boehmite binder (Dispersal P2) with a mass ratio of 95:5 and the liquid phase contained a 50:50 mass ratio of water and ethanol. These values were the same in both papers. The monoliths were coated by droplets of the solid/liquid solutions and dried at 90℃ for 2 minutes with a heating gun. This was repeated several times until the desired loading of washcoat was reached (~700 mg). Finally, the prepared monoliths were calcined at 500℃ for 2 minutes with a heat gun and calcined for 2 hours at 500℃ in a calcination oven.

3.2 Flow reactor and NO adsorption/desorption activity

By using continuous gas flow reactor studies, the PNA activity was examined under different operating conditions. There can be a broad degree of engineering freedom in flow reactor experiments including temperature, composition of the inlet gas and flow rate. For the reactor experiments the coated monoliths were placed in a horizontal quartz tube and all monoliths were wrapped with quartz wool to prevent gases from bypassing the channels. The tube was placed in a heating coil and covered with insulating material. For temperature measurements, two type-K thermocouples were inserted through the coated monoliths from the downstream end. One was placed with its tip located ca. 2 cm upstream the monolith which measured the inlet gas temperature and the other was inserted ca. 0.5 cm into the monolith to show the sample temperature. Fig. 1 shows a schematic diagram of the experimental set up for the flow reactor. Bronkhorst mass flow controllers (MFC) were used for regulating and controlling inlet gases and water feed rate was regulated by a Controlled Evaporation and Mixing (CEM) device. An MKS Multi-Gas 2030 HS FTIR spectrometer was used to monitor the outlet gases. The total gas flow rate during TPD experiments was 750 Nml min^{-1}, whereas in **Paper I** a total flow of 3500 Nml min^{-1} was used for the pre-treatment step, while for the adsorption and desorption also in **Paper I**, 750 Nml min^{-1} was used.

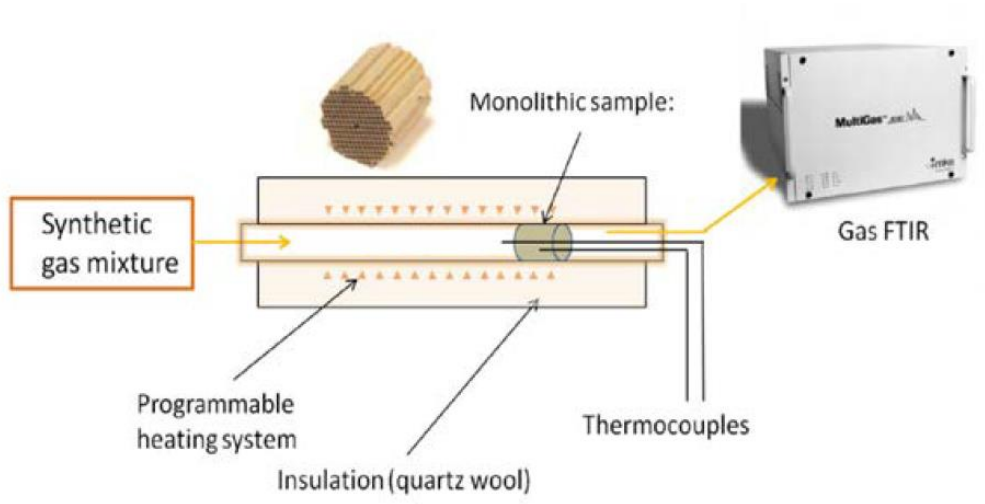

Figure 1. Schematic of the used flow reactor[51].

In both studies, a degreening step was applied in the beginning of the experiments with 1h exposure to 500 ppm NO, 8% O_2, 5% H_2O at 750°C with an argon balance (total flow 750 Nml min^{-1} at the rate of 20 °C/min).

In **Paper I**, the degreening step was followed by a pre-treatment step at 650°C for 15 min in 1% H_2, 5% H_2O with Ar balance. This pre-treatment was used in performance studies of different promoters. The effect of hydrogen pretreatment was also studied on the examined TPD by comparing two different pre-treatment conditions (I) 1% H_2, 5% H_2O with an Ar balance for 15 minutes at 650°C and (ii) 15 minutes at 750°C with Ar flush. In **Paper II** all the flow reactor results were conducted without the pre-treatment step.

In **Paper I**, the study continued by cooling down from the pre-treatment temperature (650°C) to 80°C (adsorption temperature) under 8% O_2, 5% H_2O and Ar. The storage step, consisted of 200 ppm NO, 8% O_2, 5% H_2O and Ar at 80°C for 45 min. The desorption step started by ramping up to 650°C at a rate of 20 °C/min, with the same gas composition as in storage step. In this study, the water effect was also studied with the same reactor experiment but with water absent from the gas composition, which was called dry conditions (**Paper I**).

In **Paper II** all samples were exposed to 10 cycles of NO_x adsorption/desorption after the degreening step. The storage step consisted of 200 ppm NO, 4000 ppm CO, 8% O_2, 5% H_2O and Ar at 80°C for 45 min. Next a temperature ramp up to 500°C at a rate of 20 °C/min was applied, for NO_x desorption with the same feed gas mixture. Prior to each cycle, a pre-treatment step was applied at 500°C with 8% O_2, 5% H_2O and Ar for 15 min.

3.3 Characterization techniques

3.3.1 Inductively coupled plasma sector field mass spectrometry (ICP-SFMS)

The explicit loading of the materials (La and Pd) on the Beta support were measured by ICP-SFMS for all freshly prepared samples. This analysis was performed by ALS Scandinavia AB. The basics of this method involve ionization of the sample with inductively coupled plasma and then by using a mass spectrometer (MS) these ions are separated and quantified.

3.3.2 Specific surface area analysis (BET)

According to the theory suggested by Brunauer, Emmett and Teller in 1938, the total surface area of dry and solid materials such as supported catalysts, can be measured by nitrogen physisorption[52]. The BET-method is based on various simplifications[53] including:

- All available sites have the same energy and every one of them can accommodate only one adsorbed molecule of the adsorbent.

- There can be multi-layers formation, but adsorbed molecules will not have lateral interactions.
- At any layers the adsorption and desorption rate will be equal[54].

Therefore, with respect to these assumptions, the specific surface area is measured based on the adsorbed volume of the adsorbate (N_2). This method has been useful for measuring the surface area of macroporous and mesoporous materials, but it can be deceptive for microporous materials [53]which includes zeolites as well. This is due to the difficulty to form multi-layers of the adsorbate within small pore volume materials[55]. Yet, in most literature, BET characterization has been used to compare the surface area of zeolites because the results are considered to be proportional to the pore volume[55]. In this study, a Tristar 3000 (Micromeritics) instrument with liquid N_2 at a specific temperature (-195°C) was used for the characterization. Prior to the measurements, all the fresh powder samples were degassed in N_2 overnight at 220°C under vacuum.

3.3.3 Transmission electron microscopy (TEM)

With this tool it is possible to obtain information about the morphology, structure, crystallography and elemental composition of various materials. It is possible to acquire high resolutions images of the particles down to the nanometer scale. The concept of this method is to accelerate a beam of electrons towards the powder sample. The electrons can pass through the sample with no interaction or they can be scattered by the sample atoms. The scattered electrons can gain a certain angle and be detected by a detector which is placed on the optical axis. These non-uniform collected electrons can create an image and the resolution of this image depends on the thickness of the sample. It important to have thin samples for this imaging technique, because thick samples are non-transparent due to multiple backscattered electrons[56]. In this study, TEM was employed for analyzing the noble metal particle size for different samples. The used powders were scraped from the monolith after the reactor experiments and distributed on carbon copper TEM grids (**Paper I**). For **Paper II** the fresh degreened (see Section 3.2) samples were used for analysis. The samples were analyzed with a FEI Titan 80-300 TEM.

An energy dispersive X-ray (EDX) system was used to gain information on the elemental composition in a specific area. **Paper I** includes images of reference and promoted samples with EDX mapping to investigate the distribution and location of Pd and La particles. This was carried out with a FEI Titan 80-300 microscope (same instrument as used for TEM

analysis). Basically, this method depends on excitation of the electrons from the inner shell after bombarding the sample with an electron beam. Thereafter, an electron from the outer shell will start to fill the core hole and the energy is released as an Auger electron or X-ray. The placed detector can detect the emitted X-ray value the element's characteristic energy[56].

3.3.4 X-ray photoelectron spectroscopy (XPS)

XPS analysis is an important technique to analyze the elemental compositions of a sample surface and also the chemical nature regarding the oxidation state of the atomic species. In this method, the sample is placed in an ultra-high vacuum chamber and is irradiated with high energy by a monochromic X-ray beam. The detected kinetic energy, gives the binding energy of these photoelectrons[57]. XPS analysis was used to identify the oxidation state of Pd in **Paper I** with ultra-high vacuum on a Perkin Elmer PHI 5000C ESCA system equipped with a monochromatic Al K X-ray source with a binding energy of 1486.6 eV. The reference PdO material used in this study, is from Sigma Aldrich (99.97% trace metals basis) and for reference, C1s with a binding energy of 284.8 eV was used.

3.3.5 Temperature programmed experiments

Important information regarding the oxygen interaction with available materials in different samples can be obtained with both oxidation and O_2 desorption. These analyses were carried out by placing the powder samples in a vertical quartz tube (inner diameter of 5 mm) inside an electric furnace. For regulation of gas flow and gas mixing, mass flow controllers (MFC) were connected to the system. Outlet gas compositions were measured by a Hiden HPR-20 QUI mass spectrometer. TPO in **Paper I** was conducted to observe the effect of La on the oxidation/dissociation behavior of the Pd/PdO in the PNA adsorbent. 50 mg of the fresh powder samples were loaded in the quartz tube with 20 Nml/min gas flow and Ar gas as the inert balance. The pre-treatment step involved reducing the adsorbent at 600℃ for 30 minutes in 1% H_2 and later cooling down to 100℃ under the same condition. The TPO experiment was continued by flushing with Ar at 100℃ for 25 min, followed by adding 250 ppm O_2 in Ar over the sample for 90 min. Thereafter, the oxygen consumption and subsequent formation was recorded by ramping up to 800℃ at a rate of 20℃/min, in the same gas mixture and the final step was isothermal at 800℃ for 60 min.

In **Paper II**, O_2-TPD was performed for both freshly degreened and used samples, to observe the oxygen uptake and desorption in reference and La promoted samples before and

after multiple NO_x adsorption/desorption cycles. O_2-TPD experiments started with 3 vol% oxygen in Ar at 25℃ with a gas flow rate of 20 ml/min for 5 minutes and later ramping up to 400℃ and remaining isothermal for 30 min under the same gas mixture. The experiment was followed by cooling down to room temperature with the same gas composition and remaining at these conditions for 30 min. After an hour of only Ar flushing at room temperature, the desorption step started by ramping up to 800℃ at a rate of 20℃/min in the presence of Ar.

3.3.6 In-situ DRIFT Spectroscopy

In order to characterize the surface species, diffuse Reflectance Infra-red Fourier Transformed (DRIFT) Spectroscopy was used. This is a common method for identifying various material sites by investigating adsorption of probe molecules including CO or NO. The transition between vibrational energy levels of adsorbed compounds on the surface, can produce IR from specific frequencies that can be detected by this technique[58]. In this analysis, the powder sample was placed on a porous grid in a reaction cell equipped with CaF_2A Vertex 70 spectrometer (Bruker) with a liquid nitrogen cooled MCT detector was used. The flows of inlet gases were controlled by multiple MFCs and the water vapor was controlled by a CEM (Controlled Evaporator and Mixer) system.

Paper I used DRIFTS analysis in order to study the effect of La on creating new sites for NO_x adsorption on the adsorbent and the thermal stability of these sites for the promoted sample. The samples used were the freshly calcined powder samples of the reference and La promoted sample. The experiment started with 60 min of degreening with 8% O_2, 1000 ppm NO and Ar as carrier gas at 550℃ following by a pre-treatment step at the same gas temperature with 8% O_2 in Ar for 2 hours. After cooling down to 80℃, a background spectrum was acquired in the same gas mixture. The spectra were collected while introducing 1000 ppm NO to the 8% O_2 in Ar for 30 min.

In **Paper II**, DRIFTS analysis was performed to investigate the stability of the promoted sample after multiple NO-TPD experiments in the presence of CO. Prior to this analysis, freshly prepared samples were degreened in the flow reactor (see Section 3.2). Therefore, a pre-treatment step was performed for 15 min with 8% O_2, 1% H_2O and Ar as carrier gas at 550℃. Thereafter, the chamber was cooled down to 80℃ in the same gas mixture and a background spectrum was acquired. Spectra were collected first during the introduction of 200 ppm NO, 1% H_2O and 8% O_2 for 15 min then the second spectra were collected with 200 ppm NO and 4000 ppm CO with 1% H_2O and 8% O_2 in Ar for 15 min subsequently. Furthermore, the chamber was heated up to 550℃ for 15 min for a desorption step in the same gas mixture.

These adsorption and desorption cycles were repeated and recorded three times and a new background was collected before each cycle.

4. Results and discussion

This chapter is dedicated to the presentation and interpretation of the acquired results in the two papers which had been performed with the flow reactor set up and different characterization methods. To recall, in **Paper I** the effect of different promoters on Pd/zeolite was studied for PNA processes and in addition an investigation regarding the effect of water and H_2 pre-treatment was conducted on the PNAs. Later in this study different concentrations of lanthanum as a promoter were studied to find an optimum loading of this promoter. The main focus of **Paper II** was on investigation of the adsorbent stability after multiple cold-start cycles in the presence of CO in comparison to the reference sample.

4.1 Flow reactor results

4.1.1 Study of different promoters on Pd/BEA and hydrogen pre-treatment effect

In **Paper I** three different promoters were studied including 10 wt.% Ce, Zr and La on Pd/BEA zeolite. As a reference sample, 1 wt.%Pd had been loaded on Beta zeolite support with a SAR of 38. Fig. 2 shows the quantity and the temperature range of NO_x release during the wet TPD (200 ppm NO, 8% O_2 and 5% H_2O in argon carrier) for Pd/BEA and promoted adsorbents. These experiments included a pre-treatment step prior to the main TPD experiments. Evidently, the reference sample had largest quantity of NO_x release compared to the promoted samples. However, the release temperature is in a lower range than that suitable for PNA processes (<200°C). Ce and Zr promoted samples were able to reduce the NO_x release at temperatures below the urea dosing temperature (<200°C). Interestingly, La promoted sample had a different NO_x release behavior compared with the other promoters. The presence of La could effectively shift most of the NO_x release to temperatures above 200°C (between 250-480°C). The positive behavior of La for PNA processes was also reported by Ji et al. on

Pd/Al_2O_3. They reported that addition of La to Pt/Al_2O_3, reduced desorption of NO_x at low temperatures and shifted the desorption peak to temperatures higher than 250°C[24].

The results in Fig. 2 also showed that an additional adsorption peak of NO_x appeared at temperatures from 80 to 125°C for the La promoted sample. Later in the experiment, the same wet TPD was repeated directly after cooling back to the adsorption temperature (80°C) to investigate the activity for adsorption after the first cycle. The results illustrated the same adsorption/desorption behavior as the first cycle for all adsorbents. The results in Fig. 2 clearly demonstrates that La loading, significantly increases the NO_x release temperature to more suitable desorption temperatures compared with the reference adsorbent Pd/BEA and other promoted samples. However, it should be noted that for 10%La-Pd/BEA, some of the stored NO_x is very strongly bound and requires high temperature for the desorption.

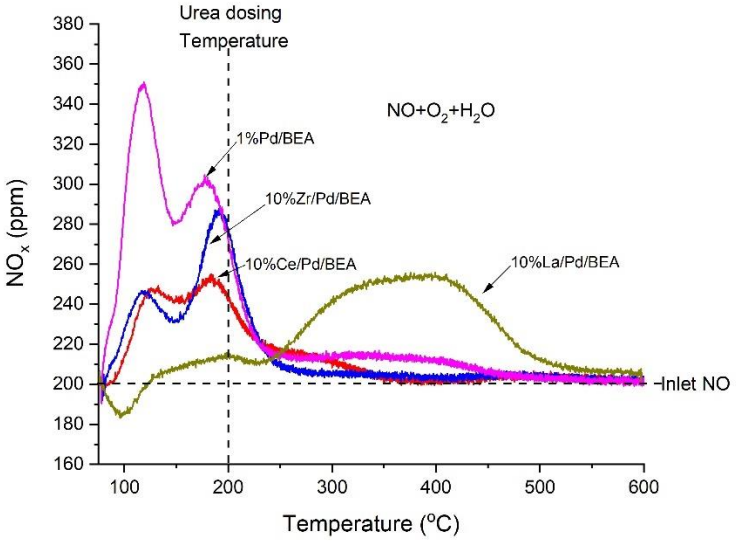

Figure 2. Wet TPD experiment (200 ppm NO, 8% O_2, 5%H_2O and Ar) over reference (1%Pd/BEA) and promoted samples.

Furthermore, in **Paper I**, the study of hydrogen pre-treatment effect was investigated on the reference sample (Pd/BEA) and 10wt.%La-Pd/BEA. Fig. 3 illustrated that H_2 pre-treatment caused a lower desorption, and thereby also NO_x adsorption, for both samples. The pre-treatment step caused a reduction of ca. 40% in desorption for the Pd/BEA sample and only ca. an 18% reduction for the La promoted sample. It is apparent that the effect of hydrogen pre-treatment was significantly smaller on the La-Pd/BEA sample. For this sample, the hydrogen pre-treatment resulted in a small shift in desorption of NO_x to lower temperature, but still above 200°C. Therefore, it was apparent that the presence of H_2 during degreening caused a decrease of adsorption capacity for NO_x (See Section 2.2.3). The La promoted sample was

less sensitive to hydrogen pre-treatment under wet condition. This was studied in greater detail with TPO characterization as discussed in Section 4.2.

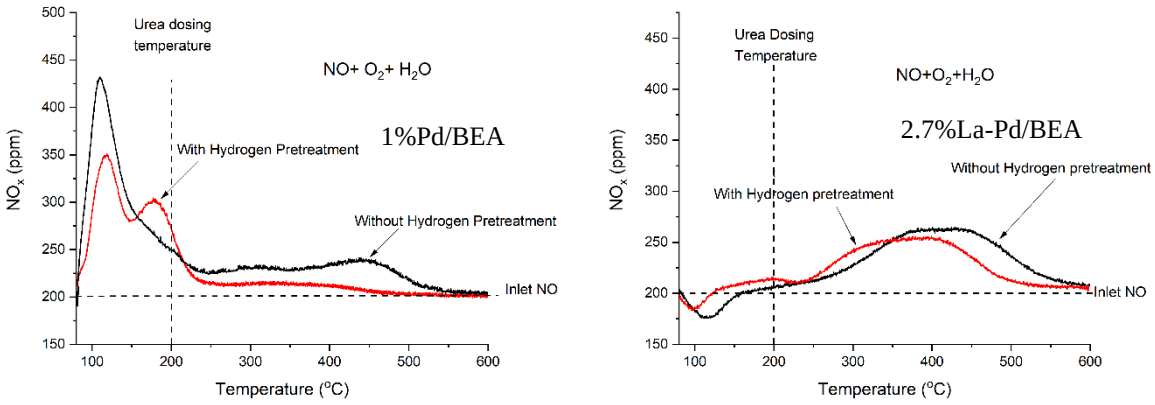

Figure 3. H_2 pre-treatment effect in wet TPD (200 ppm NO, 8% O_2, 5%H_2O and Ar).

4.1.2 Varying La loading and H_2O effect

In the second part of **Paper I**, the focus was on studying various La loadings on Pd/BEA and gaining an understanding of the effect of La on the thermal stability of the NO_x species. In this part of the study no hydrogen pre-treatment step was used before NO_x adsorption/desorption. Lanthanum as a promoter, was loaded in the range of 2.7-10 wt.% on Pd/BEA. Studying Fig. 4a reveals that loadings of 2.7 wt.% and 10 wt.% had lower NO_x desorption quantities compared with other La loading values. A possible reason for the lower NO_x storage and release for the 10 wt.% La sample could be a blockage of the pores resulting in lower Pd dispersion, and for the 2.7 wt.% sample it could be that the La loading is quite low resulting in less stable NO_x species. On the other hand, the 2.7%La-Pd/BEA sample had the most suitable temperature release for a PNA process (its release temperature was between 200 to 400°C). With 3.5, 5.4 and 7 wt.% La, a similar behavior was observed with a broad NO_x release temperature, but the temperature for maximum desorption occurred at a higher temperature (around 350°C). Moreover, for 3.5 and 7 wt.%, a small desorption peak at low temperatures (<200°C) was detected which was very minimal in the case of 5.4 wt.% La.

At the same time, all La loadings and the reference sample were studied under dry conditions to have a better understanding of the effect of H_2O on PNA processes (Fig. 4b). As it was expected, all samples had significantly larger NO_x release (and thereby more storage) in the absence of water. This fact is due to the availability of more storage sites[21-22, 25], since there is no blockage by water species. However, all the main desorption peaks were located at

temperatures lower than 200°C due to additional weakly adsorbed NO_x. But, the presence of water is inevitable in real exhaust aftertreatment application conditions.

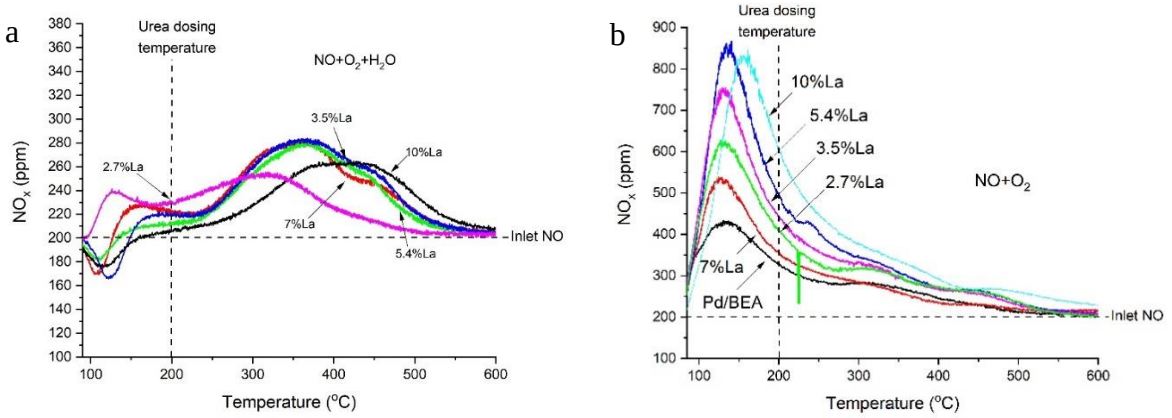

Figure 4. Comparison of different loadings of La. a) Wet TPD (200 ppm NO, 8% O_2 and 5%H_2O with Ar) without hydrogen pre-treatment b) Dry TPD (200 ppm NO, 8% O_2 and Ar) for various loadings of La without hydrogen pre-treatment.

Considering the thermal stability of the adsorbed NO_x on La promoted sample in the flow reactor results (**Paper I**), La was suggested as a promising promoter for the Pd/BEA sample. Examining different concentrations of La, it was observed that the quantity of lanthanum can shift the release temperature range. The optimum temperature range for NO_x release is above 200°C, but not too high since it will be difficult to regenerate the trap during standard operating conditions. The NOx desorption temperature depends on synthesis methods, different materials or gas compositions, aging conditions and ramping rate[24, 26, 33, 59]. Therefore, by examining the results Fig. 4a, 2.7%La-Pd/BEA was chosen to be the focus of the study in **Paper II** regarding the investigation of the effect of CO during multiple NO_x adsorption/desorption cycles. Also, in this study the objective was to examine how the order of loading La and Pd during the synthesis influenced their dispersions and ultimately the NO_x adsorption/desorption performance.

4.1.3 CO effect on sequential passive NO_x adsorption

For this study all samples were degreened (Section 3.2) and underwent adsorption at 80°C and desorption at up to 500°C with the gas mixture of 200 ppm NO, 4000 ppm CO, 1% H_2O and 8% O_2 in Ar. Fig. 5 and 6 displays the NO_x desorption profile during 10 sequential tests for the La promoted sample and 1%Pd/BEA. It can be concluded that the reference sample lost much of its NO_x release quantity during the cycles. This sample underwent a reduction in NO_x release of around 57% by the 5th cycle compared with the first cycle, and beyond 5th cycle

the degradation continued but with slower pace (10% NO_x desorption loss from 5th to 10th cycle i.e. 67% in total). This degradation was also reported by Theis et al. for Pd/BEA during multiple NO_x storage cycles with 900 ppm CO and 300 ppm H_2[28]. Interestingly, the results in Fig. 6 show a different behavior for the La promoted sample. This sample had degradation in NO_x release for about 46% from the first cycle to the 5th and had no degradation beyond 5th cycle. The desorption temperature for this sample is located from the start in a more favorable range for PNA processes, but also La helped the Pd/zeolite to reach a more stable behavior after 5th cycle. In total, the Pd/BEA sample lost 67% of the NO_x storage capacity, while the Pd-2.7%La/BEA sample only lost 46%. Correspondingly, the desorption peak at low temperatures disappeared and an adsorption peak around 160°C grew for further cycles.

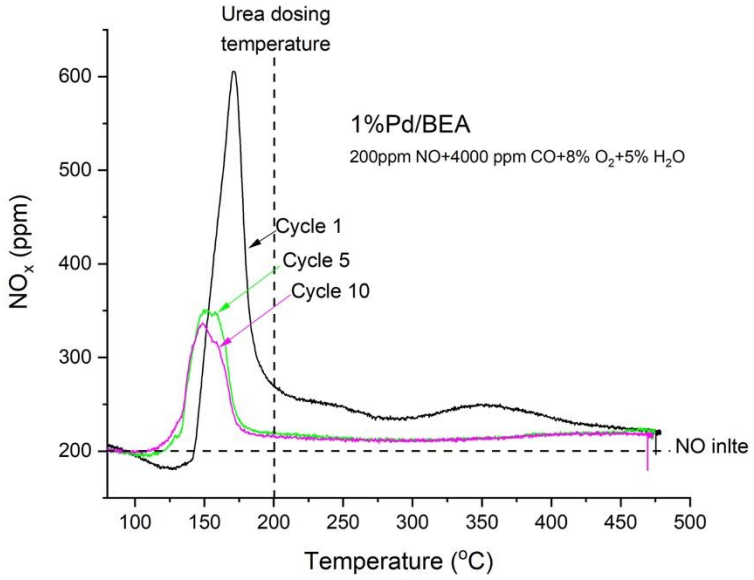

Figure 5. NO_x concentration for repeated TPD experiments with 200 ppm NO, 8% O_2, 5% H_2O and 4000 ppm CO for the reference sample.

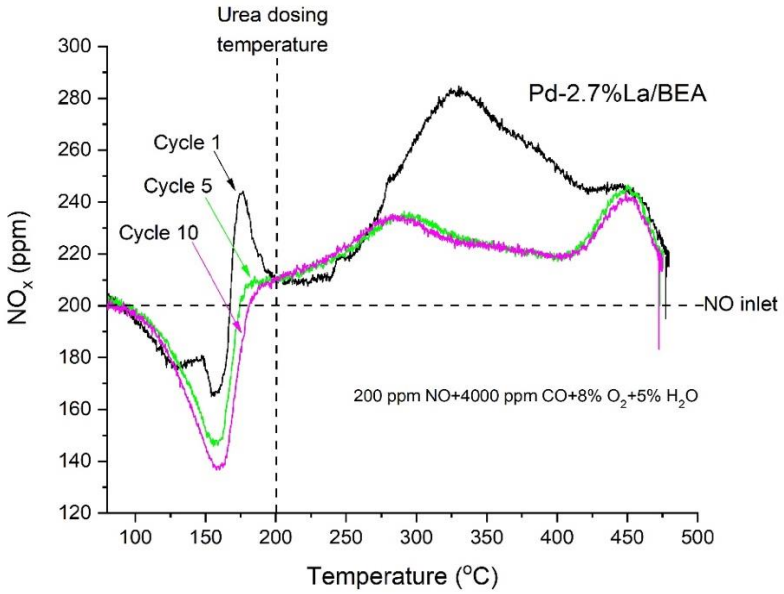

Figure 6 NO_x concentration for repeated TPD experiments with 200 ppm NO, 8% O_2, 5% H_2O and 4000 ppm CO.

4.2 Physicochemical characterization

The actual contents of Pd and La on the support were measured by ICP-SFMS (Table 1 and 2, Section 3.1.2). The surface area for all the samples were measured by using N_2 physisorption (BET). It was apparent that by increasing the La concentration, the specific surface area gets reduced. This reduction was around 30% from 0 to 10 wt. % La. This reduction was seen in pore volume as well (Table 3). This is due to the blockage of pores and the available surface area with lanthanum particles.

Table 3. BET surface areas and pore volumes.

Sample Type	SBET (m^2/g)	Pore Volume (cm^3/g)
1%Pd/BEA	597.7	0.35
2.7%La-Pd/BEA	555.1	0.32
Pd-2.7%La/BEA	540.0	0.32
3.5%La-Pd/BEA	519.0	0.31
5.4%La-Pd/BEA	477.0	0.29
7%La-Pd/BEA	427.5	0.26
10%La-Pd/BEA	414.5	0.25

TEM analysis in Fig. 7 compares the morphology of Pd particles in the reference sample and the 5.4 wt.% La promoted sample (considered an average loading for La for the range studied). In **Paper I** the used samples for this analysis were acquired after the activity test and they were scrapped off from the monolith. It should be noted that ion exchanged Pd^{2+} species cannot be detected by STEM and only an overview of the dispersed particles on the surface are possible to see with this technique. The images indicated a fairly good distribution of Pd particles in the reference sample. Fig. 7a showed that the average size of these Pd particles were around 2 to 5 nm. While, Fig. 7b showed agglomerated particles ranging from 20 to 50 nm for the 5.4%La-Pd/BEA sample. This agglomeration could explain the lower NO_x adsorption/desorption (~ 25%) ability of the La promoted sample (Fig. 2). This effect can be related to fewer available ion-exchange positions remaining, which can lead to a poorer dispersion of Pd species[21]. It has been reported in different studies that the presence of La caused occupancy of Al_2O_3 defect sites or it prevented the formation of highly dispersed oxygen-rich palladium species[24, 60].

In **Paper II** the analyzed materials consisted of freshly degreened (at 750°C for an hour with 500 ppm NO, 8% O_2, 5% H_2O and Ar) samples of 2.7%La-Pd/BEA and Pd-2.7%La-BEA to see the particles distribution. Fig. 8a indicated multiple agglomerated particles sizes between 30 to 50 nm for 2.7%La-Pd/BEA. On the other hand, an improved distribution of metals was observed for the Pd-2.7%La-BEA sample with an average particle size of 10 to 20 nm (Fig. 8b). Therefore, it has been found that the sequence of component loading can also affect the particle distribution. Therefore in Pd-2.7%La/BEA, more ion-exchange positions were available thus a better distribution of Pd was achieved[21].

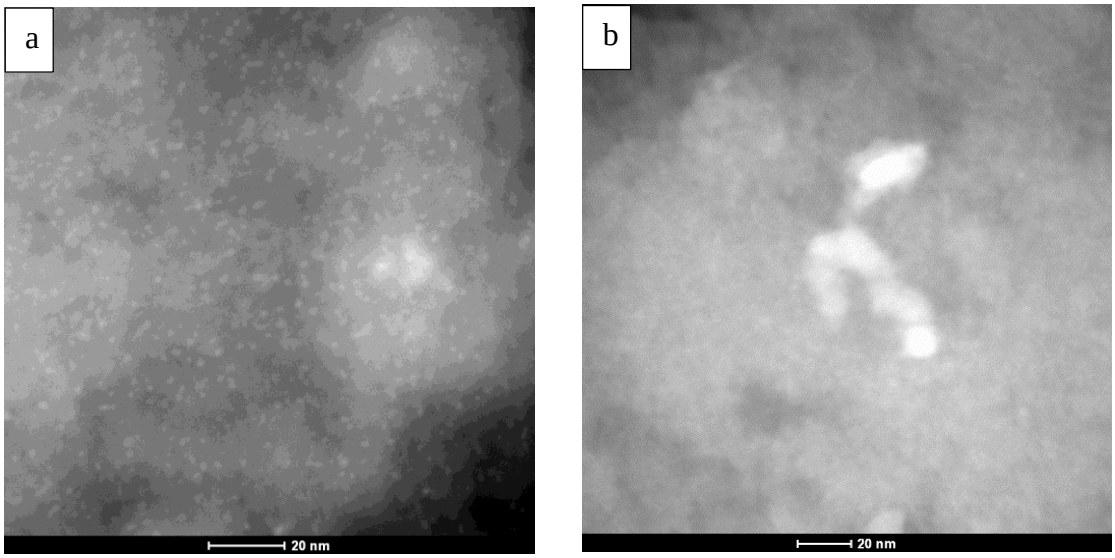

Figure 7. a) STEM images for 1%Pd/BEA at 20 nm. b) STEM images for 5.4%La-Pd/BEA sample at 20 magnifications.

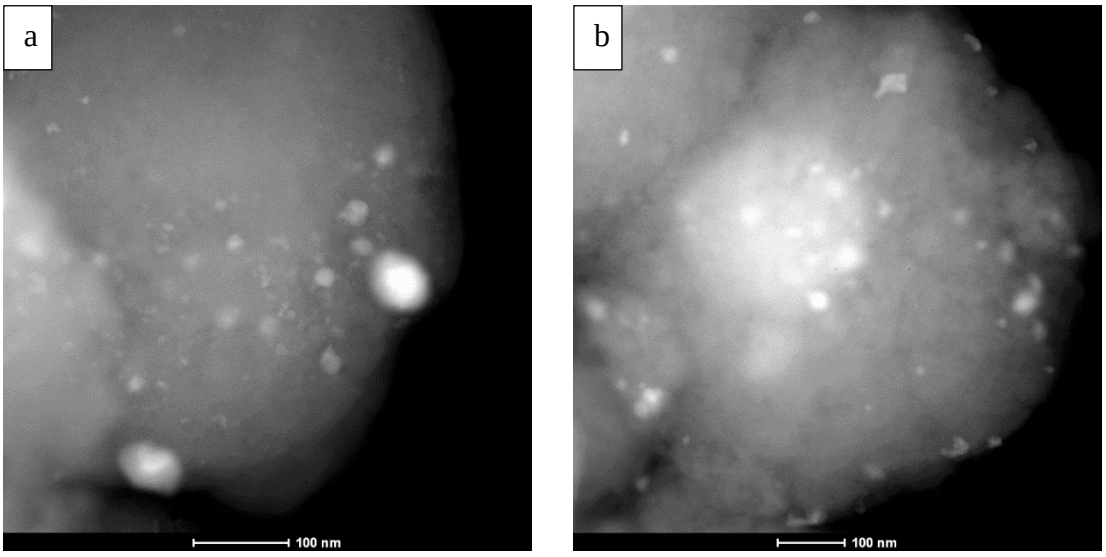

Figure 8. a) STEM images for 2.7%La-Pd/BEA at 20 nm. b) STEM images for Pd-2.7%La/BEA sample at 20 magnifications.

TPO analysis was performed in **Paper I** for freshly prepared powder samples. After the hydrogen pre-treatment step, the sample was exposed to 300 ppm O_2 in Ar at 100℃ for 90 min in order to reach a saturated state. To observe the oxygen consumption and desorption peaks, the temperature was then increased to 800℃ at a rate of 20℃/min with the same inlet gas mixture. According to the results in Fig. 9, it can be concluded that even with moderate amounts of La, the oxygen uptake became more facile because adsorption shifted to lower temperatures. Furthermore, increased the loading of La in the tested samples, gradually enhanced the stability of adsorbed oxygen. Hoost et al. claimed that the presence of La with Pd/Al_2O_3, caused a new oxidation mode for Pd which was assigned to result from $Pd\text{-}La_2O_3$ interactions[60]. To investigate the oxidation behavior of La a sample of 2.7%La-BEA was

studied with the same TPO experiment (Fig. 10). Noting that lanthanum is known to be a very stable material [61], the showed indicated no O_2 uptake and release with the La-BEA sample. It was established that the oxidation/reduction characteristics can be related to the Pd metal and interactions between Pd and La. Therefore, it is apparent that Pd is in a more thermally stable oxidized state when promoted with La, which can support the results in Fig. 2 and 3.

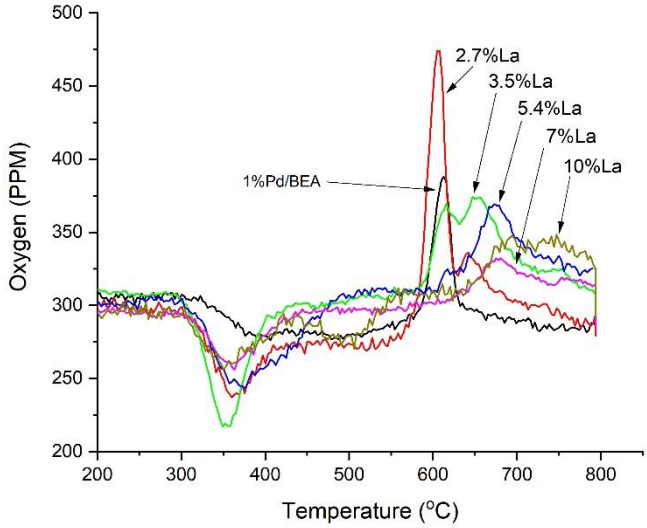

Figure 9. TPO experiment for Pd/BEA and lanthanum modified samples.

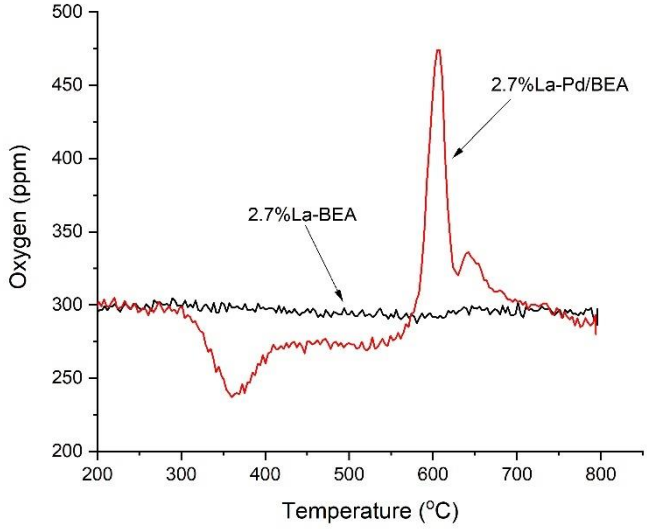

Figure 10. TPO experiment over La modified samples.

In **Paper II**, O_2-TPD was used to study the oxygen adsorption properties of Pd/BEA and Pd-2.7%La/BEA to understand the more stable behavior of the La modified sample after multiple cycles. Thus, the samples for this analysis included the degreened

(Section 3.2) fresh and the reacted samples. Fig. 11 shows the desorption peaks for the fresh degreened materials, as well as the samples used in multiple NO_x TPD cycles (in presence of high CO concentration). For the fresh La promoted sample one additional peak appeared between 300-450°C, compared to Pd/BEA sample, which can be related to adsorption of surface oxygen species on PdO_x species[62-63]. The second desorption peak (between 500-650 °C) can be assigned to the release of O_2 from decomposition of PdO_x clusters while ramping up to higher temperatures [63-64]. Meanwhile, the integrated peak area of the reacted Pd-2.7%La/BEA sample was 1.1 times higher than the fresh sample. This can be due to formation of more palladium clusters that have stronger affinity for oxygen adsorption. The peak area of the reacted Pd/BEA sample was 1.7 times higher than the fresh one. Comparison of these results indicates that the minor increase in oxygen release after the reaction from Pd-2.7%La/BEA, is caused by greater stability of this sample after multiple NO_x TPD cycles. However, for Pd/BEA the greater difference between the peak area of the fresh and reacted samples, shows that the quantity of the produced Pd clusters on the surface for Pd/BEA is much higher than that of the La modified sample. According to the literature, NO_x trapping at low temperatures is due to NO direct coordination onto ionic Pd^{2+}species[22]. Thus, having more Pd clusters on the surface decreases the amount of Pd^{2+} in the Pd/BEA sample. Therefore, the ability for NO_x uptake will gradually reduce over cycles. This fact can support the reactor results illustrated in Fig. 5 and 6.

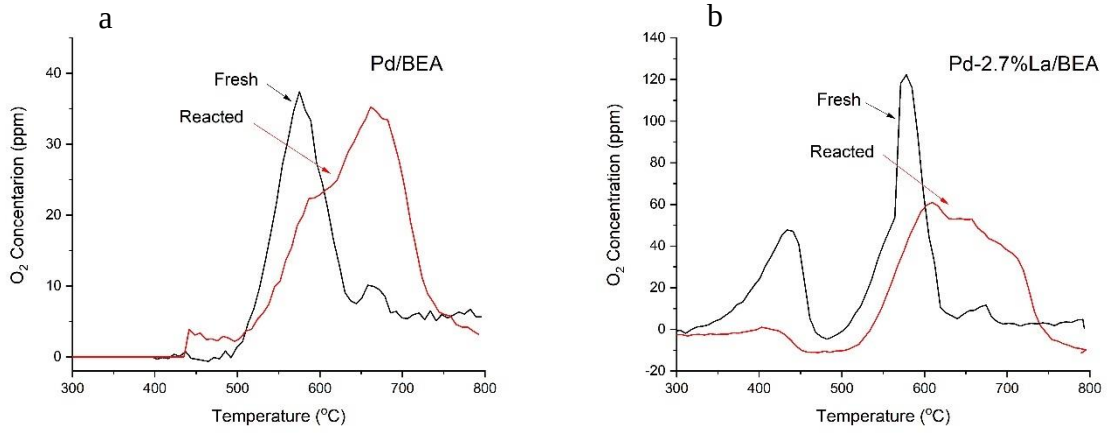

Figure 11.O_2-TPD profile of a) Pd/BEA and b) Pd-2.7%/BEA samples.

The collected spectra for XPS analysis in **Paper I** is presented in Fig. 12. XPS analysis was used to study the oxidation state of Pd in the reacted reference sample and the reacted La prompted sample (5.4%La-Pd/BEA). For having reference peaks, a commercial PdO sample was used with two Pd^{2+} peaks located at 336.9 eV($3d_{5/2}$) and 342.4 eV($3d_{3/2}$) [21] which is shown in the lower panel of Fig. 12. The Pd/BEA sample exhibited a small shift to higher binding energies and to investigate this in more detail, deconvolution was performed (Fig. 13).

For this purpose, peaks of Pd^{2+} (336.9 eV(3d5/2)[65-66] and 342.4 eV($3d_{3/2}$)) and Pd^{4+} (338.9 eV($3d_{5/2}$) and 344.6 eV($3d_{3/2}$)) was considered[25]. It can be concluded that Pd^{2+} dominates in both samples. Based on area integration, the fraction of palladium as Pd^{2+} in the La modified sample and in Pd/BEA sample was 95.2% and 84.8% respectively. Therefore, the shift of the peaks for the Pd/BEA sample is related to the larger portion of Pd present as Pd^{4+} in this sample. According to the literature, Pd^{2+} and Pd^{4+} would be in the form of PdO and PdO_2 respectively for the Pd/zeolite [25]. The higher decomposition temperature for PdO (~750°C), and stability of PdO_2 at temperatures lower than 200°C, confirms the greater thermally stability of Pd^{2+} [25, 67]. Consequently, the presence of greater quantities of Pd^{2+} in the La promoted sample, can be one of the reasons that this sample having greater thermal stability than the reference sample.

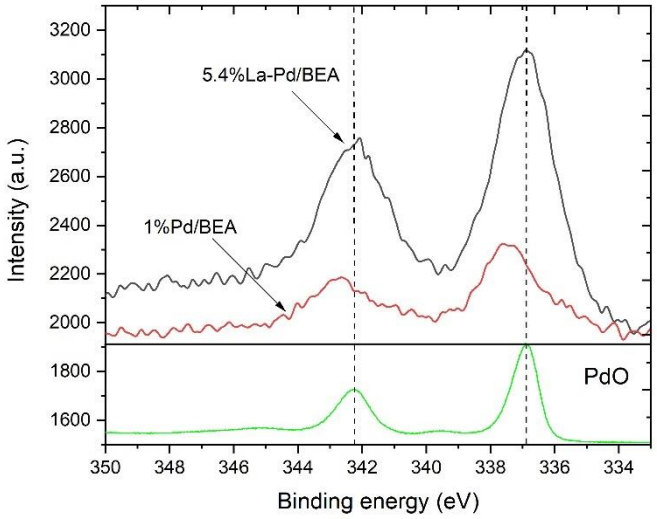

Figure 12. Pd 3d XPS spectra of the 1%Pd/BEA and 5.4%La-Pd/BEA.

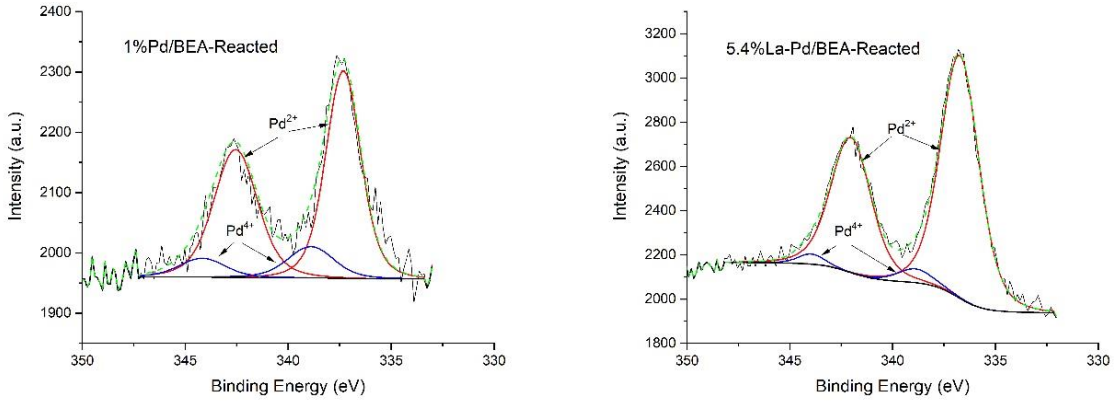

Figure 13. Deconvolution of Pd 3d XPS results for 1%Pd/BEA and 5.4%La-Pd/BEA.

4.3 DRIFT spectroscopy

DRIFTS analysis in **Paper I** provided important information about the nature and quantity of the adsorbed NO_x species on the surface of the adsorbent. In this analysis method, the spectra were collected when the freshly prepared samples were exposed to NO and O_2 at 80°C (Section 3.3.6). Fig. 14a shows the spectra collected from the Pd/BEA sample where the highest peaks appeared around 1633 and 1651 cm^{-1} which are related to NO_2 interacting with OH groups [24]. Another strong peak around 2142 cm^{-1} can be related to NO^+ on Brønsted acid sites[21-22]. Peaks at 1830 and 1876 cm^{-1} are assigned to the N = O symmetric stretch of Pd^{2+}-NO nitrosyl species and symmetric stretching vibrations of $(NO)_2$ dimers on Pd respectively[21, 26, 68]. Chelating nitrates appeared at 1589 cm^{-1} in this spectra[24, 69]. Fig. 14b illustrates the collected spectra from the 5.4wt%La-Pd/BEA sample in which the dominant peak was at 1570 cm^{-1} and according to Ji et al. this peak could be assigned to chelating bidentate nitrates [24]. Furthermore, a small peak around 1480 cm^{-1} was related to monodentate nitrates [70]. The peak which appeared at 1277 cm^{-1} was known to be bridged nitrates[71-72]. Moreover, smaller peaks at 1734 and 1876 cm^{-1} were reported as NO dimers on Pd [21] and Pd^{2+}-NO nitrosyls respectively. According to the literature, nitrates are more stable than nitrite species and will decompose at higher temperatures [17, 24, 26]. The comparison of the two spectra (Fig. 14) indicated that the presence of La on Pd/BEA enhanced the quantity of nitrate species, due to the appearance of a nitrate peak around 1277 cm^{-1} and stronger peaks at 1570 and 1480 cm^{-1}. This was also found by Ji et al with La-Pt/Al_2O_3[24]. Thus, the DRIFTS results also supported the NO_x TPD observations that more thermally stable NO bonds form on 5.4wt.%La-Pd/BEA sample, which can cause higher NO_x desorption temperature (Fig. 2).

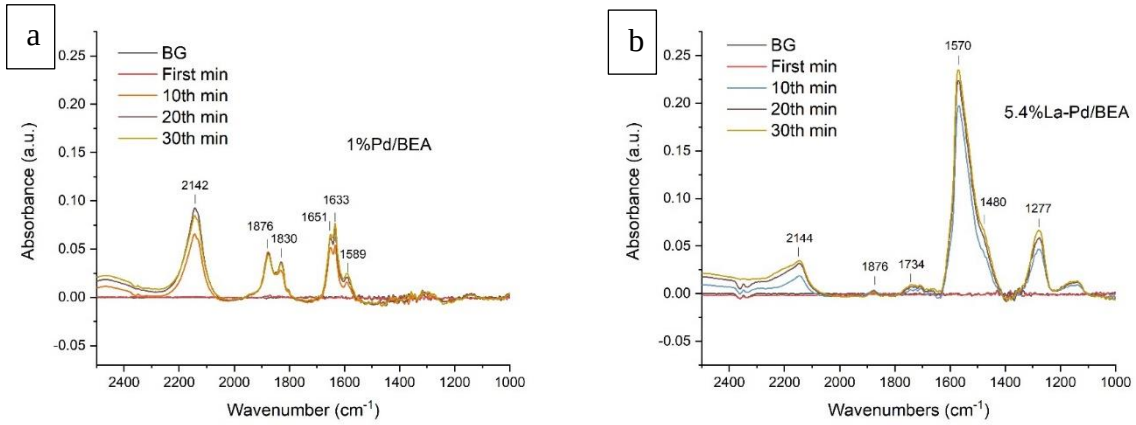

Figure 14. DRIFT spectra obtained during exposure to 1000 ppm NO and 8% O2 at 80°C with a) Pd/BEA and b) 5.4%La-Pd/BEA.

Paper II included DRIFTS analysis for degreened (Section 3.2) fresh samples and for recording the spectra, three cycles of NO-TPD was performed in the presence of H_2O (Section 3.3.6). Fig. 15 compares the NO adsorption step in each cycle for both samples. In each cycle after exposure of NO to 15 min, CO was added to the inlet gas as well. For Pd/BEA (Fig. 15a) the significant peak appeared around 1813 cm^{-1} which is assigned to linear nitrosyl species where NO is attached onto the cationic Pd^{2+} (Pd^{2+}-NO) which is placed at the exchanged sites[21, 31]. Peaks around 1633 cm^{-1} and 1653 cm^{-1} were seen in Fig. 14a as well. The strong peak at 1360 cm^{-1} can arise due to the interaction of H_2O with HNO_2[73]. Two negative peaks around 2112 cm^{-1} and 2130 cm^{-1} are assigned as linear CO on Pd^+ and linear CO on ionic Pd respectively [26, 59] . The presence of CO in each cycle can cause the formation of its linear bond with Pd^0 and the formation of $Pd^+(CO)(OH)$[74-75]. These negative peaks after the first cycle can be due to replacement of CO with NO on Brønsted acid sites[76]. Negative peaks around 3745-3784 cm^{-1} are due to consumption of hydroxyls of the zeolite structure which can occur during NO uptake[77-79]. Examining the results in Fig. 15b the strongest peak for the Pd-2.7%La/BEA sample appeared at 1543 cm^{-1} due to monodentate nitrate[71-72]. Like the DRIFTS analysis in **Paper I**, the peaks formed from the La modified sample indicates the presence of larger quantities of nitrates which confirms the higher thermal stability adsorbed NO_x on of this sample. Moreover, the comparison of Fig. 15a and b indicates that the quantity of the adsorbed species was gradually decreasing for each cycle number with Pd/BEA sample. Meanwhile, for the La modified sample this degradation was small, and the performance was more stable.

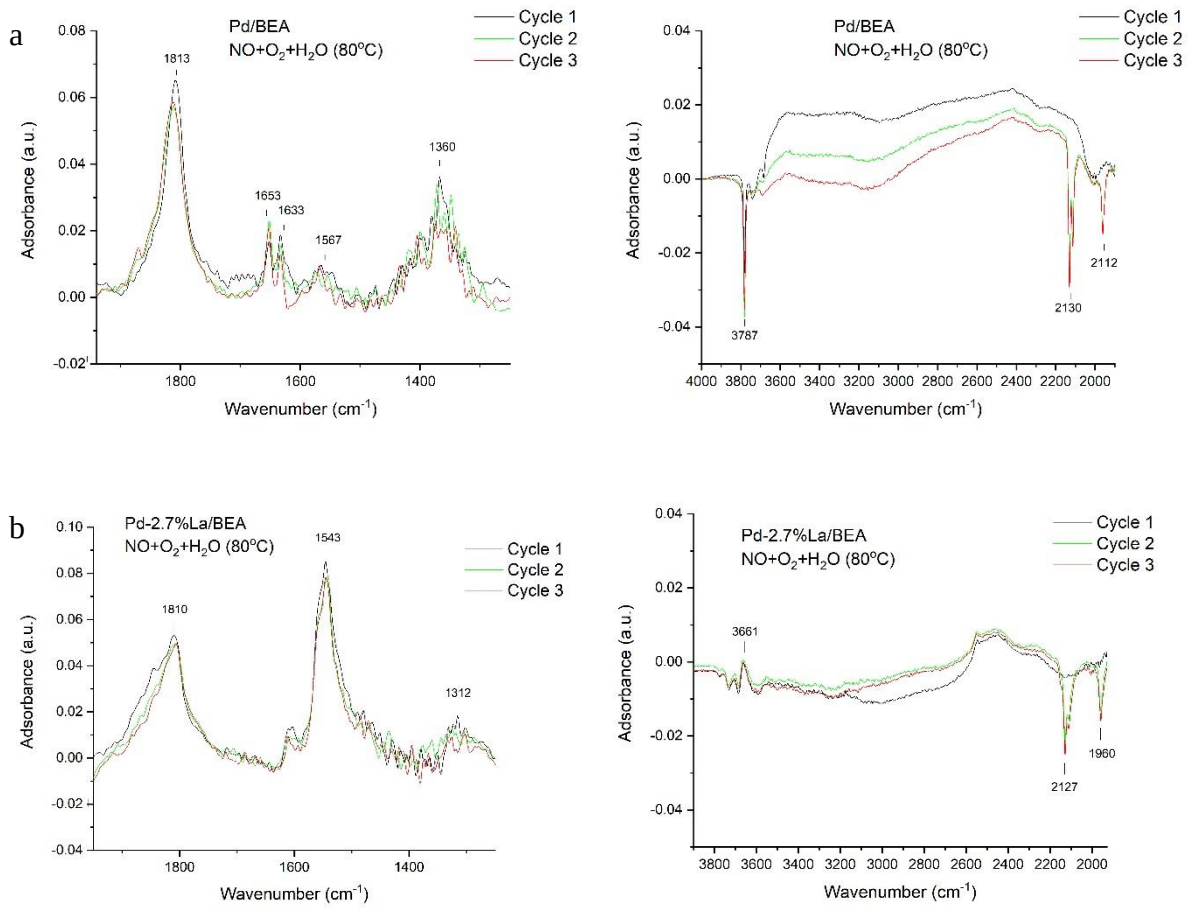

Figure 15. DRIFT spectra obtained during exposure to 200 ppm NO, 8% O_2 and 1%H_2O at 80°C with a) Pd/BEA b) Pd-2.7%/BEA.

5. Conclusions and outlook

The primary objective of this study was to fundamentally study the performance of different promoted Pd/BEA samples for passive NO_x adsorption (PNA) processes. For this purpose, ceria, zirconium and lanthanum were studied as promoters. After observing improvements in the NO_x desorption temperature window caused by La promotion, the effect of water, hydrogen-pretreatment and different La loading concentrations were investigated compared to the reference sample (Pd/BEA). Thereafter, the study was expanded to investigate the effect of CO, during multiple NO TPD cycles on the stability of the performance for the promoted and the reference sample.

In **Paper I**, the study of different promoters indicated a remarkable effect of La loading for tuning the NO_x desorption temperature window to values higher than 200°C. Meanwhile, the reference sample and other promoted Pd/BEA samples had their maximum desorption peaks at lower temperatures which is not favorable for PNA processes. The study of the effect of water on PNA processes showed that water blocked the adsorption of weakly bounded NO_x. On the other hand, hydrogen pre-treatment under wet conditions, reduced the NO_x trapping capacity for both promoted and reference samples and shifted desorption to somewhat higher temperatures. However, the La promoted sample showed less sensitivity for the effect of hydrogen pre-treatment compared to the reference sample. The flow reactor results with various La loadings, ranging from 2.7 wt.% to 10 wt.%, exhibited that 2.7 and 10 wt.% loadings had the most different desorption behavior compared to other loading values, due to insufficient loading or blocking by La, respectively. However, 2.7%La-Pd/BEA had the most favorable NO_x desorption temperature range for PNA processes. Other La concentrations, had similar desorption performance whereas, 5.4 wt.% had very minimal release before the urea dosing temperature (ca 200°C). TPO analysis displayed a more facile oxidation of La promoted samples due to shifting of the O_2 consumption peak to lower temperatures. Furthermore, the

oxygen desorption peaks were gradually shifted to higher temperatures by increasing the La loading. It was concluded that La stabilized the Pd oxidation states, which could be a reason for the greater thermal stability of NO_x species in the NO TPD experiments for the promoted sample. XPS analysis also indicated that the La modified sample had additional formation of Pd^{2+} species compared with the reference Pd/BEA sample. DRIFTS analysis showed formation of stronger peaks related to nitrate species on the La modified sample which revealed more stable surface NO_x species were formed during the adsorption step that required higher temperatures to decompose, which is in line with the flow reactor results.

In **Paper II**, the metal impregnation sequence was studied for La promoted sample. Loading of Pd prior to La on BEA support indicated that a greater quantity of NO_x release at temperatures higher than urea dosing could be achieved. TEM analysis showed a higher distribution of Pd particles for the sample with Pd loaded prior to La. Thereafter, multiple NO TPD cycling experiments were performed with the presence of CO to investigate the performance stability of the reference sample and Pd-2.7%La/BEA. The flow reactor results illustrated a stronger degrading behavior for the Pd/BEA sample while increasing the number of cycles. For this sample the NO_x release quantity was reduced by about 57% by the 5^{th} cycle and the reduction continued until the 10^{th} cycle with a slower rate. Although the La modified sample had a reduction in NO_x release of about 46% form the first to the 5^{th} cycle, this degradation stopped after the 5^{th} cycle and a more stable behavior was displayed until the last step for this sample. DRIFTS analysis also illustrated that the intensity of the formed surface NO_x species gradually decreased for the reference sample by increasing the steps while the promoted sample showed a more stable behavior after multiple cycles of NO_x adsorption/desorption with the presence of CO. O_2-TPD analysis indicated the formation of greater quantities of Pd clusters on the reference sample compared with the Pd-La/BEA sample after 10 cycles. This led to less ionic Pd sites remaining on the reference sample, which explained the reduced NO_x adsorption and desorption.

For future work, a more detailed understanding of the impact of lanthanum on performance stability of the promoted material would be beneficial. In addition, it is interesting to see if more than 10 TPD cycles are applied, how much the reference sample will loose on NO_x release and for how long the promoted material can stay stable. Furthermore, due to few studied on the kinetic modeling of PNA processes, it is interesting to have a good investigation on that part as well.

6. References

(1) Gómez-García, M.; Pitchon, V.; Kiennemann, A. Pollution by nitrogen oxides: an approach to NOx abatement by using sorbing catalytic materials. *Environment international* **2005,** *31*, 445-467.
(2) Agency, U. S. E. P. Overview of Greenhouse Gases. https://www.epa.gov (accessed 11.March.2020).
(3) Emission Standards European Union. https://dieselnet.com/standards/eu/ld.php (accessed 20.01).
(4) Arthur, A. J.; Fernandez, G. M., *Supported Metals In Catalysis (2nd Edition)*. World Scientific Publishing Company: 2011.
(5) Skalska, K.; Miller, J. S.; Ledakowicz, S. Trends in NOx abatement: A review. *Science of The Total Environment* **2010,** *408*, 3976-3989.
(6) Ji, Y.; Choi, J.-S.; Toops, T. J.; Crocker, M.; Naseri, M. Influence of ceria on the NOx storage/reduction behavior of lean NOx trap catalysts. *Catalysis Today* **2008,** *136*, 146-155.
(7) Liu, Y.; Harold, M. P.; Luss, D. Coupled NOx storage and reduction and selective catalytic reduction using dual-layer monolithic catalysts. *Applied Catalysis B: Environmental* **2012,** *121*, 239-251.
(8) Park, S. M.; Kim, M.-Y.; Kim, E. S.; Han, H.-S.; Seo, G. H2-SCR of NO on Pt–MnOx catalysts: Reaction path via NH3 formation. *Applied Catalysis A: General* **2011,** *395*, 120-128.
(9) Bosch, H.; Janssen, F., *Catalytic reduction of nitrogen oxides: A review on the fundamentals and technology*. Elsevier: 1988; Vol. 7.
(10) Fritz, A.; Pitchon, V. The current state of research on automotive lean NOx catalysis. *Applied Catalysis B: Environmental* **1997,** *13*, 1-25.
(11) Chiron, M., Effects of Motor Vehicle Pollutants on Health. In *Studies in Surface Science and Catalysis*, Crucq, A.; Frennet, A., Eds. Elsevier: 1987; Vol. 30, pp 1-10.
(12) Epling, W. S.; Campbell, L. E.; Yezerets, A.; Currier, N. W.; Parks, J. E. Overview of the Fundamental Reactions and Degradation Mechanisms of NOx Storage/Reduction Catalysts. *Catalysis Reviews* **2004,** *46*, 163-245.
(13) Bailey, D.; Solomon, G. Pollution prevention at ports: clearing the air. *Environmental impact assessment review* **2004,** *24*, 749-774.
(14) Blaszczak, R.; Cox, L.; Clean Air Technology, C., *Nitrogen oxides (NOx) : why and how they are controlled*. U.S. Environmental Protection Agency, Office of Air Quality Planning and Standards, Information Transfer and Program Integration Division, Clean Air Technology Center: Research Triangle Park, N.C., 1999.
(15) Beale, A. M.; Gao, F.; Lezcano-Gonzalez, I.; Peden, C. H.; Szanyi, J. Recent advances in automotive catalysis for NO x emission control by small-pore microporous materials. *Chemical Society Reviews* **2015,** *44*, 7371-7405.

(16) Forzatti, P.; Nova, I.; Tronconi, E. New "Enhanced NH3-SCR" Reaction for NOx Emission Control. *Industrial & Engineering Chemistry Research* **2010,** *49*, 10386-10391.
(17) Jones, S.; Ji, Y.; Bueno-Lopez, A.; Song, Y.; Crocker, M. CeO2-M2O3 Passive NOxAdsorbers for Cold Start Applications. *Emission Control Science and Technology* **2017,** *3*, 59-72.
(18) Jones, S.; Ji, Y.; Crocker, M. Ceria-based Catalysts for Low Temperature NO x storage and Release. *Catalysis Letters* **2016,** *146*, 909-917.
(19) Fridell, E.; Persson, H.; Westerberg, B.; Olsson, L.; Skoglundh, M. The mechanism for NOx storage. *Catalysis Letters* **2000,** *66*, 71-74.
(20) Mahzoul, H.; Brilhac, J. F.; Gilot, P. Experimental and mechanistic study of NOx adsorption over NOx trap catalysts. *Applied Catalysis B: Environmental* **1999,** *20*, 47-55.
(21) Mihai, O.; Trandafilović, L.; Wentworth, T.; Torres, F. F.; Olsson, L. The Effect of Si/Al Ratio for Pd/BEA and Pd/SSZ-13 Used as Passive NO x Adsorbers. *Topics in Catalysis* **2018,** *61*, 2007-2020.
(22) Chen, H.-Y.; Collier, J. E.; Liu, D.; Mantarosie, L.; Durán-Martín, D.; Novák, V.; Rajaram, R. R.; Thompsett, D. Low Temperature NO Storage of Zeolite Supported Pd for Low Temperature Diesel Engine Emission Control. *Catalysis Letters* **2016,** *146*, 1706-1711.
(23) Ren, S.; Schmieg, S. J.; Koch, C. K.; Qi, G.; Li, W. Investigation of Ag-based low temperature NOx adsorbers. *Catalysis Today* **2015,** *258*, 378-385.
(24) Ji, Y.; Bai, S.; Crocker, M. Al 2 O 3-based passive NOx adsorbers for low temperature applications. *Applied Catalysis B: Environmental* **2015,** *170*, 283-292.
(25) Zheng, Y.; Kovarik, L.; Engelhard, M. H.; Wang, Y.; Wang, Y.; Gao, F.; Szanyi, J. Low-Temperature Pd/Zeolite Passive NOx Adsorbers: Structure, Performance, and Adsorption Chemistry. *The Journal of Physical Chemistry C* **2017,** *121*, 15793-15803.
(26) Vu, A.; Luo, J.; Li, J.; Epling, W. S. Effects of CO on Pd/BEA Passive NOx Adsorbers. *Catalysis Letters* **2017,** *147*, 745-750.
(27) Yuntao Gu, R. P. Z., Yu-Ren Chen, William S. Epling Investigation of an irreversible NOx storage degradation Mode on a Pd/BEA passive NOx adsorber. *Applied Catalysis B: Environmental* **2019,** *258*, 118032.
(28) Theis, J. R.; Ura, J. A. Assessment of Zeolite-Based Low Temperature NOx Adsorbers: Effect of Reductants During Multiple Sequential Cold Starts. *Catalysis Today* **2020**.
(29) Gu, Y.; Epling, W. S. Passive NOx adsorber: An overview of catalyst performance and reaction chemistry. *Applied Catalysis A: General* **2019,** *570*, 1-14.
(30) Chen, H.-Y.; Mulla, S.; Weigert, E.; Camm, K.; Ballinger, T.; Cox, J.; Blakeman, P. Cold Start Concept (CSC™) A Novel Catalyst for Cold Start Emission Control. *SAE International Journal of Fuels and Lubricants* **2013,** *6*, 372-381.
(31) Ryou, Y.; Lee, J.; Cho, S. J.; Lee, H.; Kim, C. H.; Kim, D. H. Activation of Pd/SSZ-13 catalyst by hydrothermal aging treatment in passive NO adsorption performance at low temperature for cold start application. *Applied Catalysis B: Environmental* **2017,** *212*, 140-149.
(32) Ryou, Y.; Lee, J.; Lee, H.; Kim, C. H.; Kim, D. H. Effect of various activation conditions on the low temperature NO adsorption performance of Pd/SSZ-13 passive NOx adsorber. *Catalysis Today* **2019,** *320*, 175-180.
(33) Lee, J.; Ryou, Y.; Cho, S. J.; Lee, H.; Kim, C. H.; Kim, D. H. Investigation of the active sites and optimum Pd/Al of Pd/ZSM–5 passive NO adsorbers for the cold-start application: Evidence of isolated-Pd species obtained after a high-temperature thermal treatment. *Applied Catalysis B: Environmental* **2018,** *226*, 71-82.
(34) Ryou, Y.; Lee, J.; Lee, H.; Kim, C. H.; Kim, D. H. Low temperature NO adsorption over hydrothermally aged Pd/CeO2 for cold start application. *Catalysis Today* **2018,** *307*, 93-101.
(35) Theis, J. R. An assessment of Pt and Pd model catalysts for low temperature NOx adsorption. *Catalysis Today* **2016,** *267*, 93-109.

(36) Ji, Y.; Xu, D.; Bai, S.; Graham, U.; Crocker, M.; Chen, B.; Shi, C.; Harris, D.; Scapens, D.; Darab, J. Pt- and Pd-Promoted CeO2–ZrO2 for Passive NOx Adsorber Applications. *Industrial & Engineering Chemistry Research* **2017,** *56*, 111-125.
(37) Umeno, T.; Hanzawa, M.; Hayashi, Y.; Hori, M., Development of New Lean NOx Trap Technology with High Sulfur Resistance. SAE International: 2014.
(38) Chang, X.; Lu, G.; Guo, Y.; Wang, Y.; Guo, Y. A high effective adsorbent of NOx: Preparation, characterization and performance of Ca-beta zeolites. *Microporous and Mesoporous Materials* **2013,** *165*, 113-120.
(39) Murata, Y.; Morita, T.; Wada, K.; Ohno, H. NOx Trap Three-Way Catalyst (N-TWC) Concept

TWC with NOx Adsorption Properties at Low Temperatures for Cold-Start Emission Control. *SAE International Journal of Fuels and Lubricants* **2015,** *8*, 454-459.
(40) Ogura, M.; Hayashi, M.; Kage, S.; Matsukata, M.; Kikuchi, E. Determination of active palladium species in ZSM-5 zeolite for selective reduction of nitric oxide with methane. *Applied Catalysis B: Environmental* **1999,** *23*, 247-257.
(41) Aylor, A. W.; Lobree, L. J.; Reimer, J. A.; Bell, A. T. Investigations of the Dispersion of Pd in H-ZSM-5. *Journal of Catalysis* **1997,** *172*, 453-462.
(42) Khivantsev, K.; Gao, F.; Kovarik, L.; Wang, Y.; Szanyi, J. Molecular Level Understanding of How Oxygen and Carbon Monoxide Improve NOx Storage in Palladium/SSZ-13 Passive NOx Adsorbers: The Role of NO+ and Pd(II)(CO)(NO) Species. *The Journal of Physical Chemistry C* **2018,** *122*, 10820-10827.
(43) Adelman, B. J.; Sachtler, W. M. H. The effect of zeolitic protons on NOx reduction over Pd/ZSM-5 catalysts. *Applied Catalysis B: Environmental* **1997,** *14*, 1-11.
(44) Schmeisser, V.; Weibel, M.; Sebastian Hernando, L.; Nova, I.; Tronconi, E.; Ruggeri, M. P., Cold Start Effect Phenomena over Zeolite SCR Catalysts for Exhaust Gas Aftertreatment. SAE International: 2013.
(45) Gao, F.; Wang, Y.; Kollár, M.; Washton, N. M.; Szanyi, J.; Peden, C. H. F. A comparative kinetics study between Cu/SSZ-13 and Fe/SSZ-13 SCR catalysts. *Catalysis Today* **2015,** *258*, 347-358.
(46) Porta, A.; Pellegrinelli, T.; Castoldi, L.; Matarrese, R.; Morandi, S.; Dzwigaj, S.; Lietti, L. Low Temperature NO x Adsorption Study on Pd-Promoted Zeolites. *Topics in Catalysis* **2018,** *61*, 2021-2034.
(47) Li, W. B.; Yang, X. F.; Chen, L. F.; Wang, J. A. Adsorption/desorption of NOx on MnO2/ZrO2 oxides prepared in reverse microemulsions. *Catalysis Today* **2009,** *148*, 75-80.
(48) Theis, J. R.; Lambert, C. The Effects of CO, C_2H_4, and H_2O on the NO_x Storage Performance of Low Temperature NO_x Adsorbers for Diesel Applications. *SAE International Journal of Engines* **2017,** *10*, 1627-1637.
(49) Okumura, K.; Amano, J.; Yasunobu, N.; Niwa, M. X-ray Absorption Fine Structure Study of the Formation of the Highly Dispersed PdO over ZSM-5 and the Structural Change of Pd Induced by Adsorption of NO. *The Journal of Physical Chemistry B* **2000,** *104*, 1050-1057.
(50) Tew, M. W.; Miller, J. T.; van Bokhoven, J. A. Particle size effect of hydride formation and surface hydrogen adsorption of nanosized palladium catalysts: L3 edge vs K edge X-ray absorption spectroscopy. *The Journal of Physical Chemistry C* **2009,** *113*, 15140-15147.
(51) Azis, M. M., *Experimental and kinetic studies of H_2 effect on lean exhaust aftertreatment processes : HC-SCR and DOC*. Chalmers University of Technology: 2015.
(52) Brunauer, S.; Emmett, P. H.; Teller, E. Adsorption of Gases in Multimolecular Layers. *Journal of the American Chemical Society* **1938,** *60*, 309-319.
(53) Leofanti, G.; Padovan, M.; Tozzola, G.; Venturelli, B. Surface area and pore texture of catalysts. *Catalysis Today* **1998,** *41*, 207-219.

(54) Süheyda Atalay, G. E., *Novel Catalysts in Advanced Oxidation of Organic Pollutants*. 1st ed. 2016. ed.; Springer eBooks: 2016.
(55) Beller, M.; Renken, A.; Santen, R. A. v., *Catalysis : from principles to applications*. Wiley-VCH: 2012.
(56) Carter, C. B.; Williams, D. B., *Transmission Electron Microscopy. [electronic resource] : Diffraction, Imaging, and Spectrometry*. 1st ed. 2016. ed.; Springer International Publishing: 2016.
(57) van der Heide, P., *X-ray Photoelectron Spectroscopy : An introduction to Principles and Practices*. 1st ed. ed.; Wiley: 2011.
(58) Chorkendorff, I.; Niemantsverdriet, J. W., *Concepts of modern catalysis and kinetics*. 2nd, rev. and enlarged ed. ed.; Wiley-VCH: 2007.
(59) Wang, A.; Xie, K.; Kumar, A.; Kamasamudram, K.; Olsson, L. Layered Pd/SSZ-13 with Cu/SSZ-13 as PNA − SCR dual-layer monolith catalyst for NOx abatement. *Catalysis Today* **2020**.
(60) Hoost, T.; Otto, K. Temperature-programmed study of the oxidation of palladium/alumina catalysts and their lanthanum modification. *Applied Catalysis A: General* **1992,** *92*, 39-58.
(61) Weast, R. C.; Astle, M. J.; Beyer, W. H., *CRC handbook of chemistry and physics*. CRC press Boca Raton, FL: 1988; Vol. 69.
(62) Yu, Y.; Takei, T.; Ohashi, H.; He, H.; Zhang, X.; Haruta, M. Pretreatments of Co3O4 at moderate temperature for CO oxidation at −80°C. *Journal of Catalysis* **2009,** *267*, 121-128.
(63) Lou, Y.; Ma, J.; Hu, W.; Dai, Q.; Wang, L.; Zhan, W.; Guo, Y.; Cao, X.-M.; Guo, Y.; Hu, P.; Lu, G. Low-Temperature Methane Combustion over Pd/H-ZSM-5: Active Pd Sites with Specific Electronic Properties Modulated by Acidic Sites of H-ZSM-5. *ACS Catalysis* **2016,** *6*, 8127-8139.
(64) Simplício, L. M. T.; Brandão, S. T.; Sales, E. A.; Lietti, L.; Bozon-Verduraz, F. Methane combustion over PdO-alumina catalysts: The effect of palladium precursors. *Applied Catalysis B: Environmental* **2006,** *63*, 9-14.
(65) Otto, K.; Haack, L. P.; deVries, J. E. Identification of two types of oxidized palladium on γ-alumina by X-ray photoelectron spectroscopy. *Applied Catalysis B: Environmental* **1992,** *1*, 1-12.
(66) Kim, D. H.; Woo, S. I.; Lee, J. M.; Yang, O. B. The role of lanthanum oxide on Pd-only three-way catalysts prepared by co-impregnation and sequential impregnation methods. *Catalysis Letters* **2000,** *70*, 35-41.
(67) AzoNano Palladium Oxide (PdO) Nanoparticles – Properties, Applications. https://www.azonano.com/article.aspx?ArticleID=3404 (accessed 09.09).
(68) Hess, C.; Ozensoy, E.; Yi, C.-W.; Goodman, D. W. NO Dimer and Dinitrosyl Formation on Pd(111): From Ultra-High-Vacuum to Elevated Pressure Conditions. *Journal of the American Chemical Society* **2006,** *128*, 2988-2994.
(69) Sedlmair, C.; Gil, B.; Seshan, K.; Jentys, A.; Lercher, J. A. An in situ IR study of the NO x adsorption/reduction mechanism on modified Y zeolites. *Physical Chemistry Chemical Physics* **2003,** *5*, 1897-1905.
(70) Hadjiivanov, K. Use of overtones and combination modes for the identification of surface NO x anionic species by IR spectroscopy. *Catalysis letters* **2000,** *68*, 157-161.
(71) Westerberg, B.; Fridell, E. A transient FTIR study of species formed during NOx storage in the Pt/BaO/Al2O3 system. *Journal of Molecular Catalysis A: Chemical* **2001,** *165*, 249-263.
(72) Meunier, F.; Zuzaniuk, V.; Breen, J.; Olsson, M.; Ross, J. Mechanistic differences in the selective reduction of NO by propene over cobalt-and silver-promoted alumina catalysts: kinetic and in situ DRIFTS study. *Catalysis Today* **2000,** *59*, 287-304.
(73) Kim, Y.; Hwang, S.; Lee, J.; Ryou, Y.; Lee, H.; Kim, C. H.; Kim, D. H. Comparison of NOx Adsorption/Desorption Behaviors over Pd/CeO2 and Pd/SSZ-13 as Passive NOx

Adsorbers for Cold Start Application. *Emission Control Science and Technology* **2019,** *5*, 172-182.
(74) Khivantsev, K.; Jaegers, N. R.; Kovarik, L.; Hanson, J. C.; Tao, F.; Tang, Y.; Zhang, X.; Koleva, I. Z.; Aleksandrov, H. A.; Vayssilov, G. N.; Wang, Y.; Gao, F.; Szanyi, J. Achieving Atomic Dispersion of Highly Loaded Transition Metals in Small-Pore Zeolite SSZ-13: High-Capacity and High-Efficiency Low-Temperature CO and Passive NOx Adsorbers. *Angewandte Chemie International Edition* **2018,** *57*, 16672-16677.
(75) Zhu, H.; Qin, Z.; Shan, W.; Shen, W.; Wang, J. Pd/CeO2–TiO2 catalyst for CO oxidation at low temperature: a TPR study with H2 and CO as reducing agents. *Journal of Catalysis* **2004,** *225*, 267-277.
(76) Wang, X.; Chen, H.; Sachtler, W. M. H. Selective reduction of NOx with hydrocarbons over Co/MFI prepared by sublimation of CoBr2 and other methods. *Applied Catalysis B: Environmental* **2001,** *29*, 47-60.
(77) Gupta, A.; Kang, S. B.; Harold, M. P. NOx uptake and release on Pd/SSZ-13: Impact Of Feed composition and temperature. *Catalysis Today* **2020**.
(78) Ambast, M.; Karinshak, K.; Rahman, B. M. M.; Grabow, L. C.; Harold, M. P. Passive NOx Adsorption on Pd/H-ZSM-5: Experiments and Modeling. *Applied Catalysis B: Environmental* **2020**, 118802.
(79) Descorme, C.; Gélin, P.; Primet, M.; Lécuyer, C. Infrared study of nitrogen monoxide adsorption on palladium ion-exchanged ZSM-5 catalysts. *Catalysis Letters* **1996,** *41*, 133-138.